Engineering xxx (xxxx) xxx

Contents lists available at ScienceDirect

Engineering

journal homepage: www.elsevier.com/locate/eng

Research
Medical Engineering—Review

Nano-Engineered Platforms for Next-Generation Tumor Ablation: Integrating Local Eradication with Systemic Immunomodulation

Jinhua Luo [a,#], Bufu Tang [a,d,#], Xiaojie Zhang [a], Yun Hu [a], Shiji Fang [a,b,c], Yang Yang [a,c], Gaofeng Shu [a,c], Jingjing Song [a,b], Zhongwei Zhao [a,b], Hamid Reza Karimi [e], Minjiang Chen [a,b,c,*], Jiansong Ji [a,b,c,*]

[a] Zhejiang Engineering Research Center of Interventional Medicine Engineering and Biotechnology, The Fifth Affiliated Hospital of Wenzhou Medical University, Lishui 323000, China
[b] Cancer Center, Lishui Central Hospital, The Fifth Affiliated Hospital of Wenzhou Medical University, Lishui 323000, China
[c] Key Laboratory of Precision Medicine of Lishui City, Lishui Central Hospital, The Fifth Affiliated Hospital of Wenzhou Medical University, Lishui 323000, China
[d] Department of Interventional Radiology, Zhongshan Hospital, Fudan University, Shanghai 200000, China
[e] Department of Mechanical Engineering, Politecnico di Milano, Milano 20156, Italy

ARTICLE INFO

Article history:
Received 12 January 2026
Revised 24 March 2026
Accepted 10 April 2026
Available online xxxx

Keywords:
Tumor ablation
Nanocarriers
Tumor immune microenvironment
Pyroptosis
Ferroptosis

ABSTRACT

Minimally invasive tumor ablation techniques, such as radiofrequency ablation, microwave ablation, and cryoablation, have emerged as important modalities for treating solid tumors, owing to their advantages such as rapid recovery after treatment and reduced surgical trauma. However, their clinical efficacy remains limited by various factors, including incomplete ablation, high rates of recurrence, and an immunosuppressive tumor microenvironment. In recent years, the advent of nanoengineering strategies has provided promising avenues to overcome these limitations. Owing to their unique properties, such as tumor-targeting, controlled drug release, and immunomodulatory functions, nanocarriers not only enhance the local efficacy of ablation therapies but also modulate cell death pathways, such as pyroptosis and ferroptosis, and reprogram the tumor immune microenvironment. These effects collectively activate systemic antitumor immune responses. This review summarizes the underlying mechanisms by which nanoengineered systems augment tumor ablation, with a specific focus on key pathways through which nanocarriers synergize with ablation therapies to improve therapeutic outcomes. This review also critically assesses current limitations, including biosafety concerns and translational challenges, and discusses future perspectives, such as the development of intelligent nanocarriers and multimodal combination strategies. Ultimately, this work aims to provide theoretical insights and practical guidance for advancing the efficacy and personalization of tumor ablation therapies.

1. Overview of tumor ablation

The first modern cryosurgery system using liquid nitrogen was developed by Cooper et al. in 1961 [1]. In 1983, ultrasound-guided ethanol injection for liver tumors was pioneered by Sugiura et al. [2]. Radiofrequency ablation (RFA) was first introduced for treating patients with small liver tumors by Rossi et al. in 1993 [3]. Successful microwave ablation (MWA) for liver tumors with a size of less than 2 cm was first reported by Seki et al. from Japan in 1994 [4]. Since the advent of modern imaging technologies, image-guided thermal ablation techniques have become increasingly widespread. Ablation therapy is now commonly used to treat both primary and metastatic liver tumors, and has become routine in clinical practice [5]. Under guidance from imaging modalities such as ultrasound, computed tomography (CT), magnetic resonance imaging (MRI), or CT/positron emission tomography (PET), ablation procedures can be performed with high precision [6] (see Fig. 1 for a schematic overview of tumor ablation techniques).

Tumor ablation is a minimally invasive technique, and percutaneous thermal ablation has been widely applied for treating various solid tumors, including those of the liver, kidney, bone, and lung [7–11]. Ablation therapy eliminates all viable malignant cells within a designated target area by applying thermal energy or chemical agents [8]. Studies have demonstrated that achieving an

* Corresponding authors.
E-mail addresses: minjiangchen@wmu.edu.cn (M. Chen), jjstcty@wmu.edu.cn (J. Ji).
# These authors contributed equally to this work.

https://doi.org/10.1016/j.eng.2026.04.007

Please cite this article as: J. Luo, B. Tang, X. Zhang et al., Nano-Engineered Platforms for Next-Generation Tumor Ablation: Integrating Local Eradication with Systemic Immunomodulation, Engineering, https://doi.org/10.1016/j.eng.2026.04.007

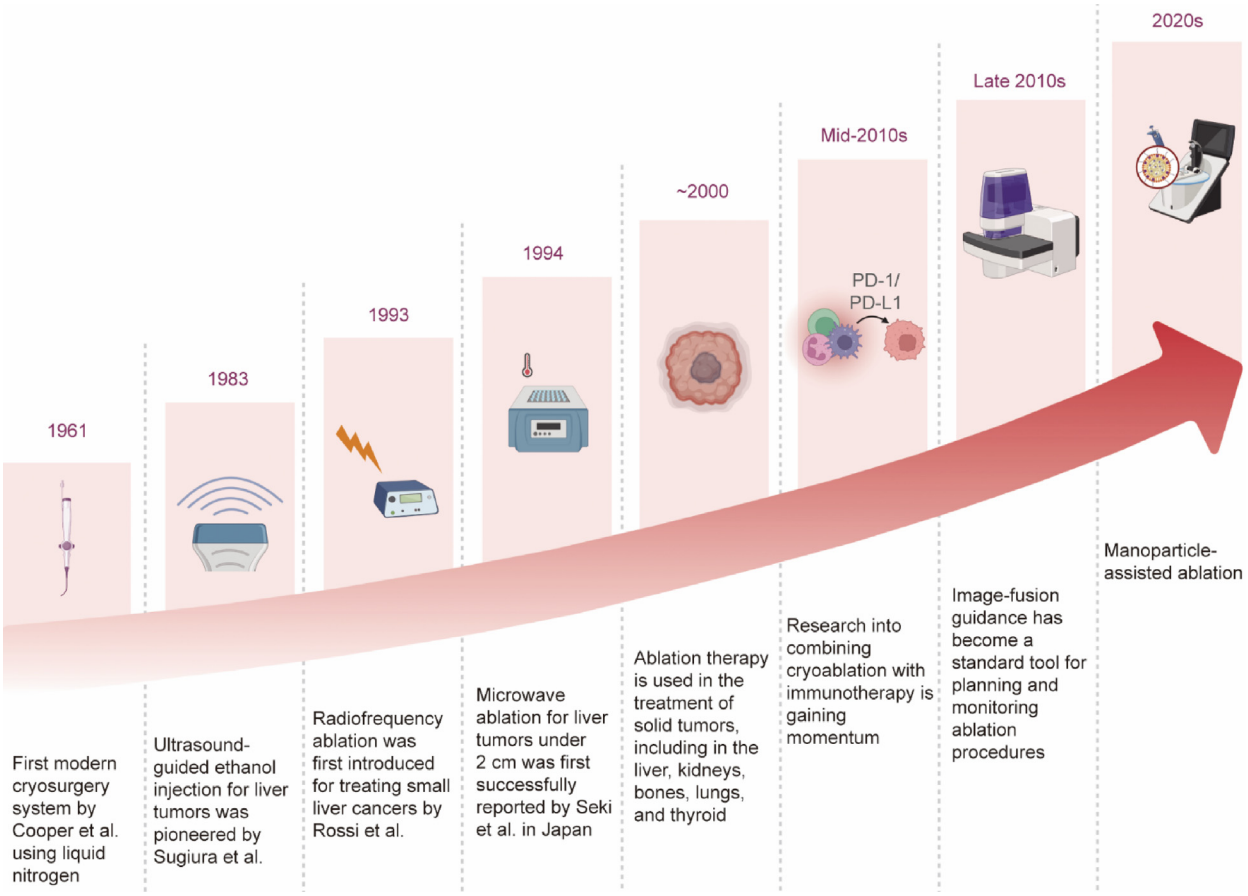

Fig. 1. A systematic overview of the evolution of tumor ablation technologies. PD-1: programmed cell death protein-1; PD-L1: programmed cell death ligand-1.

ablation margin of at least 1.0 cm into the surrounding normal tissue is critical for long-term disease-free survival in patients undergoing curative resection for hepatocellular carcinoma (HCC) [12].

One of the major advantages of tumor ablation over traditional surgery is its ability to spare a greater proportion of healthy tissue [13]. For instance, in patients with early-stage HCC, the preservation of liver function reserve is a key determinant of long-term outcomes. In such cases, tumor ablation minimizes collateral damage to the surrounding cirrhotic parenchyma, thereby offering a safer alternative [14]. Despite these advantages and widespread clinical adoption, tumor ablation is not without limitations. The following section critically examines the challenges and drawbacks that constrain its therapeutic efficacy.

1.1. Clinical applications of tumor ablation

RFA and MWA are thermal-based techniques that induce coagulative necrosis of tumors or diseased tissue by generating heat. These techniques deliver electrical or electromagnetic energy to the target tissue via electrodes or antennas embedded in specialized needles. In RFA, a high-frequency alternating current induces resistive heating of surrounding tissues via ionic agitation, resulting in localized thermal destruction around the electrode tip [6,7]. Under imaging guidance, thermal ablation techniques such as RFA, MWA, and cryoablation (Cryo) have been developed for the treatment of tumors that are difficult to resect surgically. These approaches have demonstrated high efficacy in treating both primary and metastatic malignancies [7,15,16]

Compared with RFA, MWA offers several advantages, including faster heating rates, higher intratumoral temperatures, and the ability to achieve larger zones of tumor necrosis. These characteristics make MWA particularly advantageous for treating larger tumors [17,18]. MWA can be performed via percutaneous, laparoscopic, or open surgical approaches by directly inserting a microwave antenna into the tumor site, offering flexibility in clinical application [19]. MWA generates heat by applying electromagnetic energy to biological tissues. When electromagnetic radiation in the megahertz range (typically 300 MHz to 300 GHz) interacts with tissue, polar molecules, such as water, attempt to realign with the oscillating electric field. This molecular friction generates heat, resulting in coagulative necrosis. On the basis of power deposition and tissue characteristics, ablation zones larger than 5 cm can be achieved [20,21]. Compared with other thermal ablation modalities, MWA offers several advantages, including a shorter ablation time, lower susceptibility to heat-sink effects, larger and more uniform ablation zones, and the ability to maintain higher intratumoral temperatures [20,22,23]. These features contribute to its potent cytotoxicity, minimal invasiveness, and growing popularity in the treatment of various solid tumors, including lung cancer, HCC, and colorectal cancer [24–26].

Cryo involves cycles of rapid freezing and thawing. During the procedure, high-pressure argon or nitrogen gas is delivered to the chamber at the tip of a cryoprobe, where it expands and rapidly cools. This cooling induces cell death through coagulative necrosis, caused by direct cellular injury from extreme cold, as well as by vascular stasis and ischemia in the targeted tumor tissue [27,28]. Percutaneous Cryo has been shown to completely eradicate renal cell carcinoma (RCC) lesions up to 4 cm in diameter. For nonsurgical candidates with tumors up to 7 cm, CT-guided Cryo remains a viable alternative, offering high efficacy with relatively low com-

plication rates [29–31]. Cryotherapy is now widely used to treat renal and musculoskeletal tumors, primarily because of its key advantage of compatibility with multiple imaging modalities, particularly unenhanced CT imaging. This flexibility significantly improves procedural safety, particularly when tumors are located near anatomically critical structures where the risk of collateral damage is high [15,28,32].

However, emerging evidence suggests that image-guided percutaneous Cryo not only provides substantial pain relief but also offers local tumor control, potentially eliminating the need for additional interventions such as radiotherapy or surgical resection, thereby reducing the overall treatment burden and cost [33–35]. Energy-based tumor ablation, or thermal ablation, refers to the application of extreme temperatures, either high or low, to induce irreversible cellular injury, ultimately leading to apoptosis and coagulative necrosis in tumors [36,37].

In terms of both efficacy and safety, intraoperative visibility of the ablation zone is crucial for optimizing outcomes. Laser interstitial thermal therapy (LITT) is fully compatible with MRI, enabling real-time thermographic monitoring and precise control of the ablation volume. This feature makes LITT particularly suitable for treating central nervous system tumors, where precision is critical [38,39]. Irreversible electroporation (IRE) is a novel nonthermal ablation technique that induces tumor cell death through the delivery of high-voltage electrical pulses. Unlike thermal methods, IRE preserves surrounding vascular and ductal structures, making it especially promising for tumors adjacent to major blood vessels or bile ducts. Clinical studies have demonstrated that, when combined with surgery in patients with pancreatic cancer, IRE can significantly extend overall survival (20 vs 13 months) and alleviate cancer-associated pain [40,41]. Additional advantages of ablation therapies include shorter hospital stays and cost-effectiveness compared with conventional options [37,42] (see Fig. 2 for a classification of tumor ablation therapies).

1.2. Limitations of tumor ablation

Despite the expanding indications and increasing use of thermal ablation in clinical practice, it still carries a significant risk of damaging adjacent structures, particularly the skin, intestines, and neural tissues. Thermal ablation at temperatures between 60 and 100 °C typically results in immediate coagulative necrosis; however, tissue vaporization and carbonization may occur when the temperature exceeds 110 °C, which can adversely affect the therapeutic efficacy of ablation [36,43]. Although prolonged exposure of tumor cells to sublethal hyperthermia (40–60 °C) can lead to irreversible cellular damage, temperatures exceeding 60 °C induce rapid protein denaturation and mitochondrial dysfunction, and inhibit DNA replication. These thermal effects can occur almost instantaneously. However, image-guided percutaneous tumor ablation techniques, such as RFA, may also cause unintended thermal injury to surrounding normal tissues, including the skin, bowel, and nerves [44–47]. Achieving a target temperature at a single point within the tumor does not necessarily guarantee complete ablation. In fact, spatially heterogeneous heating throughout the entire ablation zone, rather than a uniform temperature distribution, is typically observed [48,49].

When evaluating the efficacy of Cryo combined with imaging techniques, it is essential to account for factors such as the position of the lethal isotherm, the number of freeze–thaw cycles, and the rate of thawing. Studies have shown that, during Cryo, the distance between the visible ice ball margin and the actual lethal isotherm in normal renal parenchyma may be only a few millimeters. Consequently, a safety margin of approximately 6 mm between the ablation zone and adjacent normal renal tissue is generally recommended for patients with RCC [50–52]. This narrow margin inevitably increases the technical complexity and demands greater precision from the operator. Studies have shown that misplacement of cryoprobes may compromise the accuracy of early prostate cancer biopsies under MRI guidance and reduce the likelihood of achieving complete tumor coverage during Cryo procedures [50].

Studies have shown that when tumors are located in critical regions, such as near the gastrointestinal tract or hepatic hilum, the use of thermal ablation may be associated with an increased incidence of major complications [53]. In the treatment of pulmonary malignancies using MWA, complications such as pneumothorax, hemoptysis, and severe skin burns have been reported [54,55]. In addition, percutaneous thermal ablation is limited by the quality of imaging guidance and, in some cases, by complex anatomical structures or difficult-to-access tumor locations. Most patients with HCC are diagnosed at an advanced stage, when tumors are typically large and no longer amenable to curative surgery. In such cases, ablation procedures become technically challenging and may offer limited therapeutic benefit [56–58]. A comprehensive comparison of the advantages and disadvantages of each ablation modality discussed is provided in Table 1 [6,7,20,21,28,32,37,40,41,59–63].

To overcome these limitations, researchers have turned to nanotechnology. The next section introduces nanocarriers and their antitumor mechanisms, which form the foundation for combination strategies with tumor ablation.

2. Antitumor mechanisms of nanocarriers

2.1. Targeting delivery

Nanocarriers, which are engineered structures typically ranging from 1 to 100 nm, offer unique physicochemical properties that enable efficient drug encapsulation, targeted drug delivery, and controlled drug release [64,65]. Nanocarriers possess several advantageous properties, including small particle size, a controllable morphology, and ease of surface functionalization. These features enable efficient encapsulation, adsorption, or covalent conjugation of both hydrophilic and hydrophobic drug molecules [66]. Moreover, nanocarriers provide a protective microenvironment for therapeutic agents to overcome biological barriers [67].

In recent years, a broad spectrum of drug delivery systems (DDSs) has been developed to increase the efficacy of cancer therapy. DDSs can increase the accumulation of anticancer drugs at tumor sites, reduce the dosing frequency, and lower the risk of multidrug resistance, ultimately improving the overall efficacy of cancer therapy [65,68,69]. Among DDSs, liposomes are extensively investigated as platforms for targeted drug delivery [70,71].

Passive targeting leverages the enhanced permeability and retention (EPR) effect associated with the tumor vasculature, promoting the accumulation of liposomes at tumor sites. In contrast, active targeting is achieved by functionalizing the liposome surface with ligands, such as small molecules, peptides, or monoclonal antibodies, that specifically bind to receptors overexpressed on cancer cells. This targeted approach significantly improves the precision and therapeutic efficiency of drug delivery [72,73].

Liposomes tend to accumulate in tissues with high vascular permeability, such as tumors and sites of inflammation, as well as in organs with discontinuous endothelium, including the liver, spleen, and bone marrow [74]. Taxane-based chemotherapeutic agents, such as paclitaxel and docetaxel, have become cornerstone drugs in the treatment of various cancers, including breast cancer, because of their potent antitumor activity. However, their high hydrophobicity poses significant challenges for their clinical administration. To overcome their poor aqueous solubility, lipid-based solvents have traditionally been employed as carriers

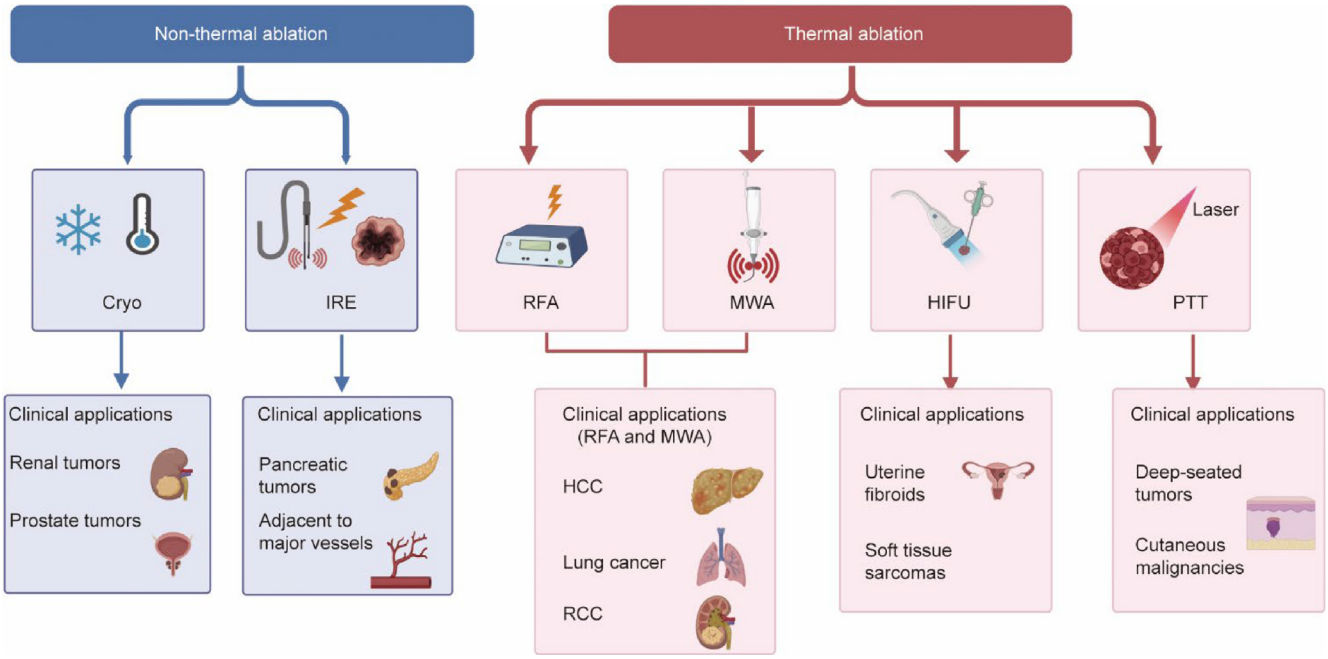

Fig. 2. A systematic overview of tumor ablation technologies. Ablation is divided into non-thermal ablation (Cryo and IRE) and thermal ablation (RFA, MWA, high-intensity focused ultrasound (HIFU), and photothermal therapy (PTT)). Each modality is clinically applied to specific tumor types: RFA and MWA are widely used for HCC, lung cancer, and RCC; Cryo is commonly employed for renal and prostate cancer; IRE is particularly suited for pancreatic tumors and tumors adjacent to major vessels; HIFU is primarily used for uterine fibroids and soft tissue sarcomas.

Table 1
Summary of the advantages and disadvantages of tumor ablation technology.

Technique name	Main principle	Typical application scenarios	Advantages	Disadvantages	Refs.
RFA	Uses high-frequency electrical current to cause ionic agitation and frictional heat (70–100°C), leading to coagulative necrosis of tumor tissue	Liver cancer (primary, metastatic); lung cancer (early-stage, inoperable); RCC; bone tumors	Mature technology with ample long-term efficacy data; relatively simple operation; widely available; definitive efficacy for tumors < 3 cm.	Heat sink effect; limited ablation zone; risk of damage to adjacent hollow organs, bile ducts, and nerves	[6,7,37]
MWA	Uses microwave electromagnetic fields to cause water molecules to rotate rapidly, generating frictional heat	Liver cancer; lung cancer; RCC; larger volume tumors (>3 cm); highly vascular tumors	Fast heating, high temperatures, shorter ablation time; larger, more uniform ablation zone; less affected by heat sink effect; effective for highly vascular tumors	Can produce a wider "charring zone;" technically demanding: requires skill to avoid accidental injury	[20,21,37]
Cryo	Circulates ultra-cold cryogens through probes to rapidly freeze tissue below –40°C, forming an "ice ball," followed by thawing; destroys cells through freeze–thaw cycles	RCC; prostate cancer; lung cancer; bone tumors; tumors near intestines, bile ducts	Excellent visualization: clear "ice ball" margins easy to monitor; significant analgesic effect, minimal intra/post-operative pain; preserves scaffold structures, low bleeding risk; can induce "cryo-immunity" effect	Long procedure time; risk of hemorrhage during thawing; potential for systemic "cryoshock" reaction; expensive equipment	[28,32]
IRE	Delivers high-voltage, short electrical pulses to create numerous irreversible nanopores in cell membranes, inducing apoptosis; a non-thermal mechanism	Suitable for tumors in "no-touch" zones near vital structures; liver cancer near hepatic hilum; renal cancer near renal hilum; pancreatic cancer	Non-thermal ablation: perfectly preserves vessels, bile ducts, nerves, et al.; sharp, clear ablation margins; unaffected by heat sink effect; rapid tissue healing	Risk of cardiac arrhythmia, requires synchronized electrocardiogram (ECG) monitoring; currently limited to smaller tumors (typically < 3 cm)	[40,41,59]
HIFU	Focuses low-energy ultrasound waves from outside the body onto an internal target, generating high temperatures (60–100°C) causing instantaneous coagulative necrosis	Mainly used for soft tissue tumors in solid organs; uterine fibroids; adenomyosis; prostate cancer; pancreatic cancer; bone tumors	Truly non-invasive: no puncture wound, no radiation; fast recovery, low risk of complications; real-time temperature monitoring possible	Long treatment duration; highly dependent on acoustic pathway; requires extremely still patient positioning	[60,61]
Multimodal ablation	Technical synergy: Combines two or more different ablation techniques or uses different modes within the same technology (e.g., dual-frequency RFA and multi-probe MWA) sequentially or concurrently to overcome single-technique limitations	Large or irregular tumors (>5 cm); tumors adjacent to critical structures; highly vascular tumors; recurrent or residual tumors	Synergistic effect: increases rate of complete tumor necrosis; toxicity reduction: reducing severe complication risks; overcomes limitations: effectively circumvents inherent drawbacks of single techniques; offer more treatment options	Technically complex: requires highly skilled operators proficient in multiple techniques; high treatment cost: lack of high-level evidence	[62,63]

[75,76] (see Fig. 3 for a systematic overview of the antitumor mechanisms of nanocarriers).

Nucleic acid-based therapeutics have emerged as a major research focus because of their high efficiency and target specificity. However, their clinical application is hindered by poor cellular uptake and susceptibility to enzymatic degradation. To exert their therapeutic effects, nucleic acid drugs require an effective delivery system to facilitate cellular entry and protect them from degradation [77,78].

Liposomes can encapsulate nucleic acid drugs, thereby shielding them from nucleases and increasing their stability *in vivo*. In addition, liposomal carriers can facilitate the transport of nucleic acid drugs across biological barriers to reach diseased tissues, thereby improving delivery efficiency and enabling precision therapy [73,79].

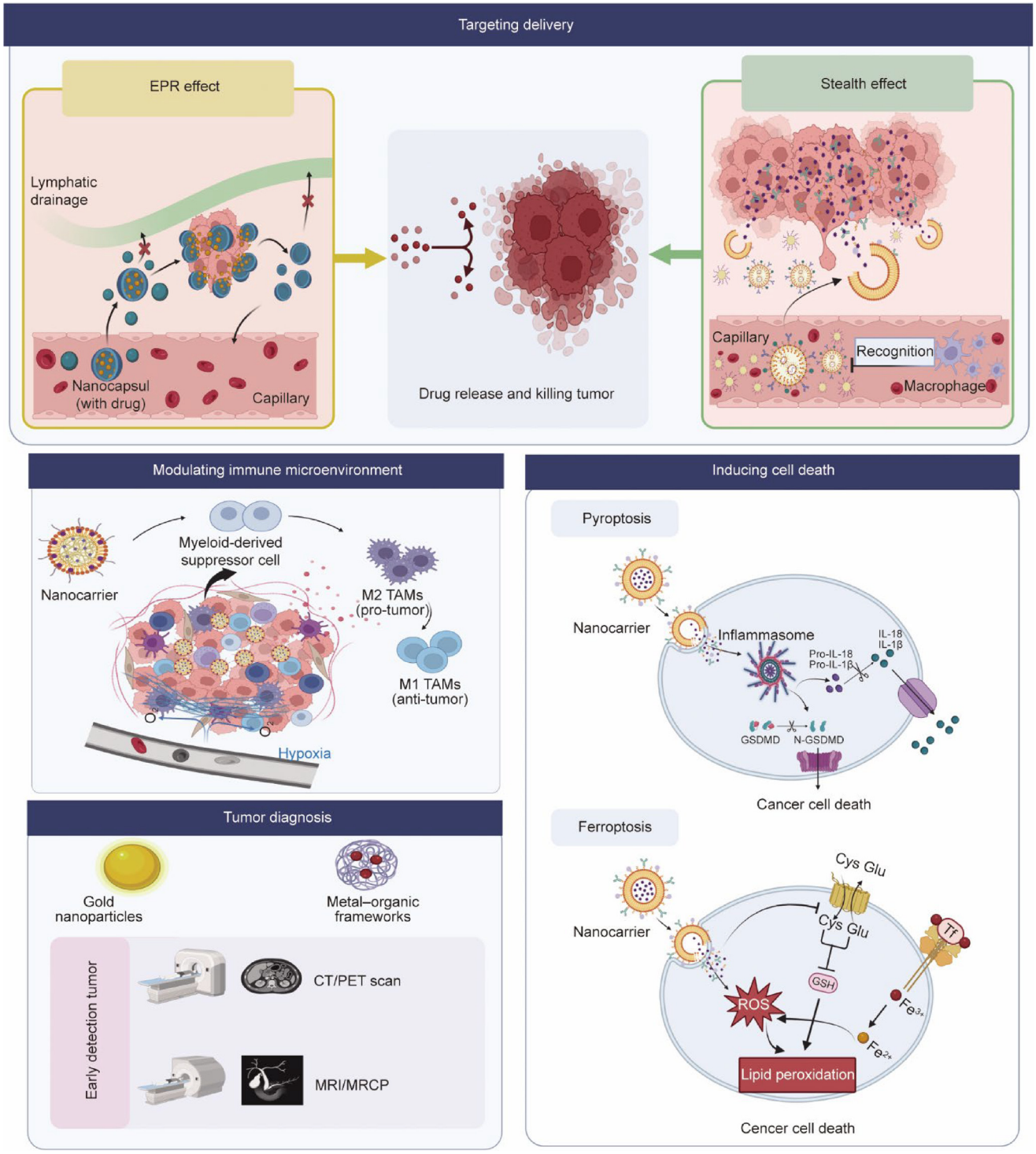

Fig. 3. A systematic overview of the antitumor mechanisms of nanocarriers. TAM: tumor-associated macrophage; MRCP: magnetic resonance cholangiopancreatography; IL-18: interleukin-18; IL-1β: interleukin-1β; GSDMD: gasdermin D; *N*-GSDMD: N-terminal domain of GSDMD; ROS: reactive oxygen species; Cys: cysteine; Glu: glutamic acid; GSH: glutathione; Tf: transferrin.

In 1987, Felgner et al. [80] demonstrated that cationic liposomes formulated with the synthetic lipid 1,2-dioleoyl-3-trimethy lammonium-propane could efficiently complex with nucleic acids, confirming the potential of liposomes as gene delivery vehicles. The world's first small-interfering RNA (siRNA)-based drug, patisiran (Onpattro®), was approved by the US Food and Drug Administration (FDA) to treat hereditary transthyretin (TTR)-mediated amyloidosis with polyneuropathy. By utilizing a lipid nanoparticle (LNP) delivery system, patisiran enables targeted delivery of the siRNA to hepatocytes, thereby reducing the production and deposition of TTR amyloid and slowing disease progression [81,82].

2.2. Modulating the immune microenvironment

The tumor immune microenvironment is an ecological system composed of diverse immune cell populations, cancer-associated fibroblasts, endothelial cells, pericytes, and various other tissue-resident stromal cells [83]. These cellular components play crucial roles in cancer initiation and progression [84]. Tumor cells actively coordinate a tumor microenvironment (TME) by recruiting and reprogramming nonmalignant host cells, and by remodeling the vasculature and extracellular matrix (ECM). Consequently, these nontumor components have emerged as promising targets for cancer immunotherapy [85,86]. For example, chimeric antigen receptor T cell therapy has demonstrated remarkable success in the treatment of hematologic malignancies [87]. Despite significant advances in the field of cancer immunotherapy, most patients still fail to achieve durable clinical benefits from currently available treatments [88]. For example, significant advances have been made in immune checkpoint blockade (ICB) therapy, but most patients fail to achieve durable clinical benefits because of unresolved factors such as dendritic cell (DC) dysfunction and the inherently immunosuppressive nature of the TME [88–90].

Nanocarriers have been developed to facilitate immune modulation, offering distinct advantages for targeted drug delivery to solid tumors [91,92]. By encapsulating therapeutic agents within nanoscale carriers, this approach can significantly prolong the drug circulation time and reduce the systemic toxicity commonly associated with free drugs [93]. By exploiting features of the TME, including the leaky vasculature, acidity, and hypoxia, nanocarriers achieve passive targeting via the EPR effect, extending intratumoral drug retention [94–96]. These nanoscale platforms have demonstrated promising tumor-selective therapeutic effects via TME reprogramming [97,98].

Recent advances in nanocarrier-based cancer immunotherapy have offered promising, tumor-selective strategies for inhibiting tumor growth and metastasis [99].

As introduced in Section 2, nanocarriers modulate the tumor immune microenvironment through multiple mechanisms (see Fig. 4 for a schematic overview).

2.2.1. Targeting immune cells

An immunosuppressive TME (iTME) supports tumor development by impairing antitumor immune responses. Key immunosuppressive cell populations, including tumor-associated macrophages (TAMs), myeloid-derived suppressor cells (MDSCs), and regulatory T cells (Tregs), play central roles in shaping the iTME [100–102]. These cell subsets exhibit distinct phenotypes and secrete various immunoregulatory factors that interact with cancer cells, thereby promoting tumor growth and metastasis. Such an abnormal immune landscape significantly compromises immune surveillance and cytotoxicity, ultimately enabling tumor cells to evade immune surveillance [103]. Among the various immunosuppressive cell types in the TME, TAMs are considered major contributors to tumor progression and immune tolerance [104,105].

Macrophages are considered to have both beneficial and harmful functions in the context of cancer, as they possess both tumoricidal and tumor-promoting properties [106]. They can be polarized into either classically activated M1-like macrophages or alternatively activated M2-like macrophages [107]. M1 macrophages exert antitumor effects by secreting proinflammatory cytokines, promoting tumor cell necrosis, and increasing immune cell infiltration into the TME. In contrast, M2 macrophages, typically known as TAMs, are widely recognized for their tumor-supportive functions. They contribute to cancer progression by promoting angiogenesis, recruiting immunosuppressive cells, and facilitating tumor cell proliferation and metastasis under hypoxic conditions [108,109].

Notably, the TME itself regulates macrophage recruitment and polarization, thereby shaping their protumoral behavior. This ability has led to increasing interest in developing functional nanocarriers designed to repolarize TAMs, aiming to shift their phenotype from the tumor-promoting M2 type to the tumor-inhibiting M1 type, a strategy that holds great promise for increasing the efficacy of cancer immunotherapy [94,106]. Given the high plasticity of macrophages in the TME, nanoparticles (NPs) can be engineered to specifically target TAMs and modulate their polarization. For instance, iron oxide NPs, which have already approved by the FDA for clinical use, have been shown to be able to reprogram M2-like TAMs toward the proinflammatory M1 phenotype, thereby enhancing antitumor immune responses [110]. The therapeutic potential of targeting tissue-resident macrophages extends beyond oncology. In cardiovascular diseases, modulating microglia, the resident macrophage population in the brain, has been shown to attenuate neuroinflammation, reduce sympathetic overactivity, and improve outcomes in patients with hypertension and myocardial infarction [111]. Another study employed a bimetallic Ca/Zn nanoagonist, PZH/Zn@CaNA, which similarly repolarized M2-like TAMs into the M1 phenotype. In addition, PZH/Zn@CaNA can be combined with MWA to produce a robust antitumor immune effect [112]. This strategy effectively modulated the iTME and enhanced T-cell-mediated immune responses, thereby synergistically improving the efficacy of chemotherapy.

DCs play a key role in activating the immune system in anticancer immunotherapeutic strategies. As professional antigen-presenting cells, DCs possess a remarkable capacity to initiate robust and long-lasting immune responses [113,114]. The antitumor immune response critically depends on specialized subsets of conventional DCs, which capture tumor antigens and transport them to draining lymph nodes [115]. There, they provide essential costimulatory signals for T-cell priming and activation, ultimately inducing cytotoxic T lymphocytes (CTLs) and eliciting tumor-specific immune responses. However, the tumor itself can shape the TME, significantly impairing DC function. This dysfunction compromises antigen presentation and T-cell activation, facilitating immune evasion and weakening the overall antitumor immune response [94,115,116]. To combat the highly iTME associated with B-Raf proto-oncogene, serine/threonine kinase (*BRAF*)-mutant melanoma, one study developed lipid-coated calcium phosphate NPs for the efficient delivery of the *BRAF*V600E tumor antigen [117]. This NP-based vaccine promoted DC maturation and increased their antitumor functionality, thereby eliciting a potent antigen-specific T cell response and effectively inhibiting tumor growth. The experimental results demonstrated that vaccination with lipid-calcium-phosphate (LCP) NP-based formulations significantly suppressed the progression of aggressive *BRAF*-mutant melanoma. Li et al. [118] introduced a "nano-epidrug" termed macrophage membrane-coated FIDAS-5-loaded MnO_2 nanoparticle with anti-PD-L1 (MFMP), which is composed of hollow mesoporous manganese dioxide (MnO_2) NPs, FIDAS-5 as a methionine adenosyltransferase 2A (MAT2A) inhibitor, a macrophage membrane, and an anti-programmed cell death ligand-1 (PD-L1) antibody (aPD-

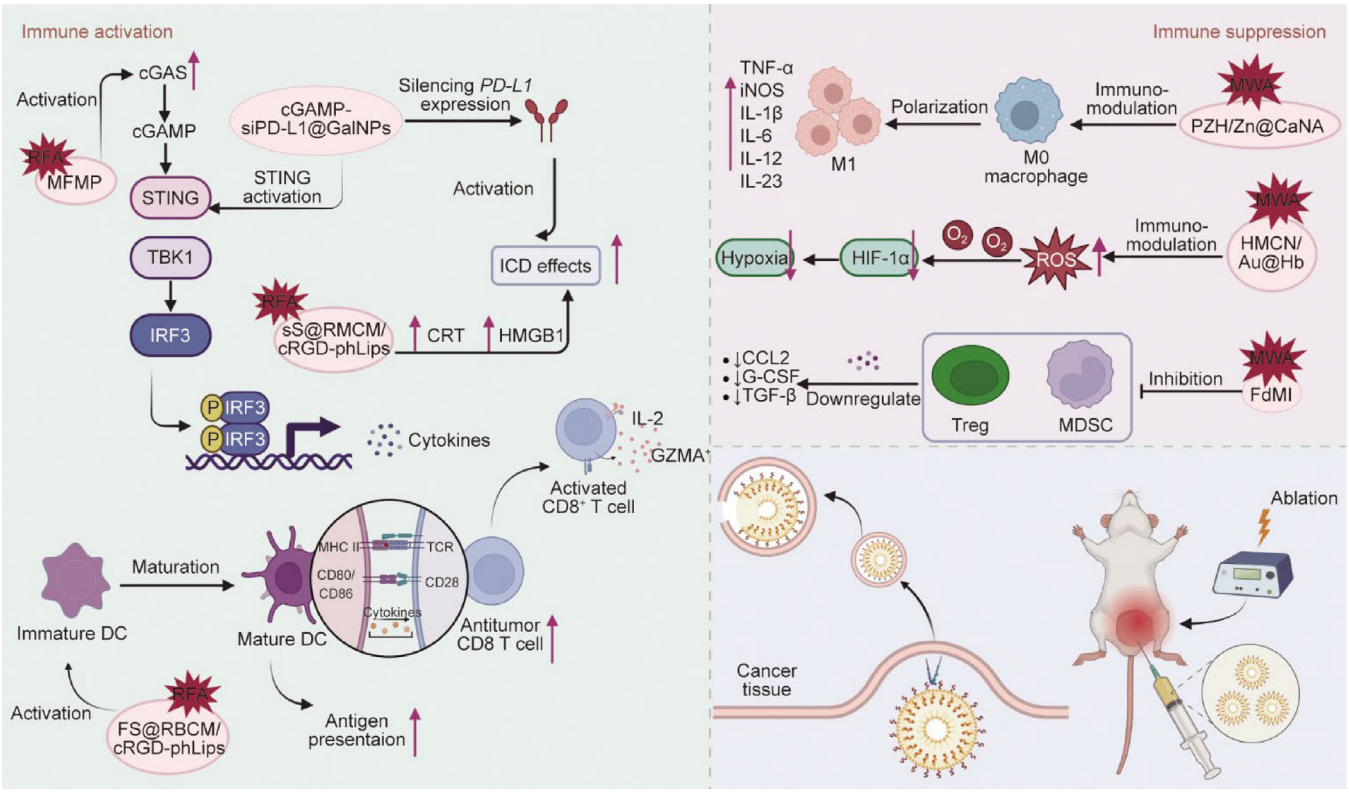

Fig. 4. Nanocarriers synergize with ablation techniques to kill tumor cells by reprogramming the TME and enhancing antitumor immunity. MFMP: macrophage membrane-coated FIDAS-5-loaded MnO_2 nanoparticle with anti-PD-L1; cGAS: cyclic GMP–AMP synthase; cGAMP: cyclic GMP–AMP; STING: stimulator of interferon genes; TBK1: TANK binding kinase 1; IRF3: interferon regulatory factor 3; siPD-L1: small interfering RNA targeting programmed cell death ligand 1; GalNP: galactose-installed nanoparticles; ICD: immunogenic cell death; CRT: calreticulin; HMGB1: high-mobility group box 1; RBCM: red blood cell membrane; cRGD: cyclic arginine–glycine–aspartic acid; phLips: pH-sensitive liposomes; GZMA: granzyme A; MHC II: major histocompatibility complex class II; TCR: T-cell receptor; CD8: cluster of differentiation 8; TNF-α: tumor necrosis factor-α; iNOS: inducible nitric oxide synthase; PZH: Pien Tze Huang; CaNA: calcium-based nanoagonist; HMCN: hollow mesoporous carbon nanoparticles; HIF-1α: hypoxia-inducible factor-1α; CCL2: C–C motif chemokine ligand 2; G-CSF: granulocyte colony-stimulating factor; TGF-β: transforming growth factor-β; Treg: regulatory T cell; MDSC: myeloid-derived suppressor cell; FdMI: fucoidan-decorated metal-organic framework incorporating manganese and ionic liquid.

L1). MFMP initially reverses immune suppression via PD-L1 inhibition. MFMP also disassembles in the TME, releasing FIDAS-5 and Mn^{2+}. Mn^{2+} promotes the restoration of the stimulator of interferon genes (STING) pathway. These changes increase the antigenicity of HCC cells to promote their recognition and killing by cytotoxic T cells. Tang et al. [119] constructed a nanocarrier codelivery system loaded with superparamagnetic iron oxide (SPIO) and fatty acid-binding protein 5 (FS@RBCM/cRGD-phLips). This platform demonstrated strong potential for stimulating DC-based immunotherapy by promoting the maturation of bone marrow-derived DCs (BMDCs) and activating both T-cells and macrophages. Importantly, this platform increased RFA efficacy by improving biocompatibility. Yu et al. [97] introduced a nanovaccine, maleimide cross-linked Pluronic F127–chitosan NP-encapsulated Astragalus polysaccharide (AMNP). AMNP was proposed to strengthen the effects of immunotherapy. AMNP recognizes immunogenic tumor antigens generated from Cryo, activates DCs, modulates T-cell differentiation, and enhances the antigen-specific CTL response through multiple immune-related pathways.

2.2.2. Targeting hypoxia

Hypoxia contributes to the formation of the TME by inducing mitochondrial stress and progressively increasing reactive oxygen species (ROS) levels, ultimately leading to T-cell exhaustion [120–122]. The TME, and particularly within tumor cells, is characterized by hypoxia and high concentrations of the reducing agent glutathione (GSH), which impedes ROS generation and accumulation, thereby severely limiting ROS-mediated oxidative damage [123].

Notably, immunotherapy outcomes remain suboptimal among patients with triple-negative breast cancer (TNBC), primarily because of the hypoxia-induced "cold" TME, characterized by poor T-cell infiltration and low immunogenicity, which collectively promote the invasion and metastasis of breast cancer cells, resulting in reduced clinical responses to immunotherapies [124,125].

Alleviating hypoxia within the TME has been shown to increase antitumor immune responses [126]. One study synthesized a nitric oxide (NO)-based molecular probe, BN-O, with a second switchable near-infrared imaging signal that transitions from an "off" to an "on" state in response to hypoxia in the TME [127]. Under hypoxia, BN-O can trigger photodynamic therapy (PDT), promoting immunogenic cell death (ICD). This dual-modal therapy synergistically activated the cyclic GMP–AMP synthase (cGAS)/STING pathway, thereby eliciting a robust antitumor immune response.

Another study developed a multifunctional nanoplatform, SP94-PB-SF-Cy5.5 NPs, to achieve targeted drug delivery, the controlled release of shikonin (SF), and effective photothermal therapy (PTT) [128]. This nanoplatform incorporates Prussian blue (PB), which has catalase (CAT)-like activity and can alleviate hypoxia in the TME by decomposing endogenous hydrogen peroxide (H_2O_2). Zhang et al. [129] designed ultrasmall gold NP-anchored hollow mesoporous carbon NPs (HMCNs) loaded with hemoglobin (Hb) to serve as a MWA nanosensitizer (HMCN/Au@Hb). Upon microwave irradiation, HMCN/Au@Hb can alleviate hypoxia in the microenvironment, which improves the antitumor response.

Low-pH insertion peptides (pHLIPs) that exploit the acidic conditions of the hypoxic TME have also been employed for selective

drug delivery to tumor tissues, thereby improving drug resistance, increasing bioavailability, and modulating the TME [130]. In addition, pHLIPs have been utilized for the targeted delivery of radioactive isotopes to hypoxic tumor cells. For example, pHLIPs labeled with radionuclides such as ^{64}Cu and ^{18}F demonstrated excellent imaging capabilities and selectively accumulated in hypoxic regions, enabling precise localization of hypoxic tumors [131,132].

As introduced in Section 2.2, nanocarriers modulate the tumor immune microenvironment through multiple mechanisms, as shown in the schematic overview in Fig. 4. Beyond immune modulation, nanocarriers can directly trigger specific cell death pathways that increase the immunogenic effects of ablation. Section 2.3 explores two such pathways, namely, pyroptosis and ferroptosis, and the unique advantages of applying nanocarriers to induce them.

2.3. Induction of cell death

2.3.1. Nanocarrier-mediated induction of pyroptosis

Pyroptosis is a form of proinflammatory programmed cell death characterized by cell swelling, large bubble-like protrusions, plasma membrane rupture, and the release of proinflammatory intracellular factors, such as interleukin-1β (IL-1β) and interleukin-18 (IL-18) [133]. This process is primarily mediated by the activation of inflammasome complexes, which trigger the cleavage of gasdermin D (GSDMD) by inflammatory caspases. The cleaved N-terminal domain of GSDMD oligomerizes and inserts into the plasma membrane, forming functional pores that execute a lytic form of cell death. Thus, pyroptosis is considered a gasdermin (GSDM)-mediated cell death pathway [134].

In both humans and mice, caspases in the canonical (caspase 1 (CASP1)) and noncanonical (CASP4, also known as CASP11 in mice, and CASP5) inflammasome pathways specifically cleave GSDMD at the linker region between its N- and C-terminal domains. This cleavage is a critical step in the formation of membrane pores and the initiation of pyroptosis [135–137]. Pyroptosis plays a critical role in both anti-infective and antitumor immunity. As a proinflammatory form of programmed cell death, pyroptosis causes the release of intracellular proinflammatory mediators, such as IL-1β and IL-18, which stimulate innate and adaptive immune responses [134,136].

Mechanistically, pyroptosis induces the release of damage-associated molecular patterns (DAMPs), contributing to inflammasome activation and promoting effective immune responses [138]. Ling et al. [112] designed a multifunctional bimetallic Ca/Zn nanoagonist (PZH/Zn@CaNA) that can be combined with MWA to induce pyroptosis. This nanoagonist increases calcium levels in cells in the TME to activate pyroptosis, which results in the release of DAMPs, thereby triggering immune activation. Yu et al. [139] developed self-cascading pyroptosis-STING initiators composed of cobalt fluoride (CoF_2). This CoF_2 nanocatalyst triggers GSDM-mediated pyroptosis. This process involves the induction of mitochondrial damage and the subsequent release of mitochondrial DNA (mtDNA). The released mtDNA is thought to activate the cGAS/STING pathway, thereby augmenting the antitumor immune response [139]. Zhang et al. [140] designed a copper-bacteriochlorin nanosheet (Cu–tris(2-benzimidazolyl)borane (TBB)) that induces pyroptosis. Cu–TBB nanosheets have been shown to potently trigger pyroptosis *in vitro* and *in vivo* through the release of Cu^+ and TBB in the TME [140]. Xiao et al. [141] described a nanomedicine (PCL@GSK-diABZI/aPD-1) that combines with granzyme B to trigger pyroptosis through delivery of the DNA methylation inhibitor GSK-3484862 into tumor cells. Chen et al. [142] engineered the nanomedicine acid-activatable nanophotosensitizer (ANPS) to specifically target distinct endocytic signaling pathways and trigger pyroptosis. ANPS activates phospholipase C, which specifically elicits gasdermin E (GSDME)-mediated pyroptosis via membrane perforation [142].

Furthermore, pyroptosis-induced DAMP release increases the recruitment and activation of tumor-infiltrating immune cells. The expression of GSDME has been shown to increase the phagocytic activity of TAMs and promote the infiltration and cytotoxic function of natural killer (NK) cells and cluster of differentiation 8 $(CD8)^+$ T cells, collectively contributing to tumor suppression [143,144].

Another study engineered a tumor-specific NP (NP-NH-D5) to activate the pyroptosis pathway [145]. Pyroptosis-associated DAMPs stimulate pattern recognition receptors on innate immune cells, leading to the activation of downstream NK and T cells. This process increased antitumor immune responses and significantly improved the efficacy of anti-CD274 antibody (CD274/PD-L1) ICB therapy in 4T1 breast and Pan02 pancreatic ductal adenocarcinoma tumor models. Wang et al. [146] designed a nanomedicine (DOX@FRMSN-O2), which acts as an MWA amplifier and consists of O_2-binding mesoporous silica NPs and doxorubicin. It can be combined with MWA to amplify the nonclassical pyroptosis pathway. MWA amplification increases the O_2 ratio to reverse the MWA-induced aggravation of the hypoxic TME and improve MWA outcomes [146] (see Fig. 5 for a schematic overview of pyroptosis pathways).

Beyond cataloging nanocarriers that induce pyroptosis, it is critical to address a fundamental question: What unique advantages do nanocarriers offer over conventional small-molecule inducers in triggering pyroptosis? The answer lies in the distinct physicochemical properties of nanoscale platforms, which enable spatiotemporal control and multimodal intervention that small molecules alone cannot achieve.

Nanocarriers enable high local concentrations of reactive ions at the subcellular scale. For instance, the bimetallic Ca/Zn nanoagonist (PZH@CaNA) [112] and CoF_2 nanocatalysts [139] leverage their nanoscale architecture to deliver a burst of Ca^{2+} or Co^{2+} ions specifically within the TME. This localized ion overload, achieved through pH-responsive dissolution or cellular uptake, can efficiently trigger mitochondrial damage and subsequent GSDM activation. In contrast, small-molecule ionophores lack such tumor-selective accumulation and risk systemic toxicity.

Nanocarriers facilitate mitochondria-specific targeting, which is particularly important in the context of pyroptosis induction given the central role of mtDNA release in activating the cGAS/STING pathway [139]. Surface functionalization with mitochondrion-targeting moieties (e.g., triphenylphosphonium) allows nanocarriers to deliver their payloads directly to this organelle, amplifying mtDNA stress and subsequent pyroptotic cell death—a level of precision unattainable with free drugs.

The ability to codeliver synergistic agents in a spatiotemporally controlled manner distinguishes nanocarriers from simple drug combinations. For example, the nanomedicine PCL@GSK-diABZI/aPD-1 [141] simultaneously delivers a DNA methylation inhibitor to sensitize tumor cells and an immune checkpoint inhibitor to sustain the subsequent antitumor response. This "all-in-one" delivery approach ensures that both agents act on the same cell at the optimal time, maximizing the likelihood of triggering GSDM-mediated pyroptosis while minimizing off-target effects.

Nanocarriers can exploit endocytic pathway hijacking to activate pyroptosis through mechanisms distinct from those of small molecules. The ANPS platform [142] was engineered to specifically engage phospholipase C signaling via receptor-mediated endocytosis, leading to membrane perforation and GSDME cleavage. This mechanism-based activation, which relies on the recognition of cell surface receptors at the nanoscale, offers a level of cell-type specificity that small-molecule pyroptosis inducers often lack.

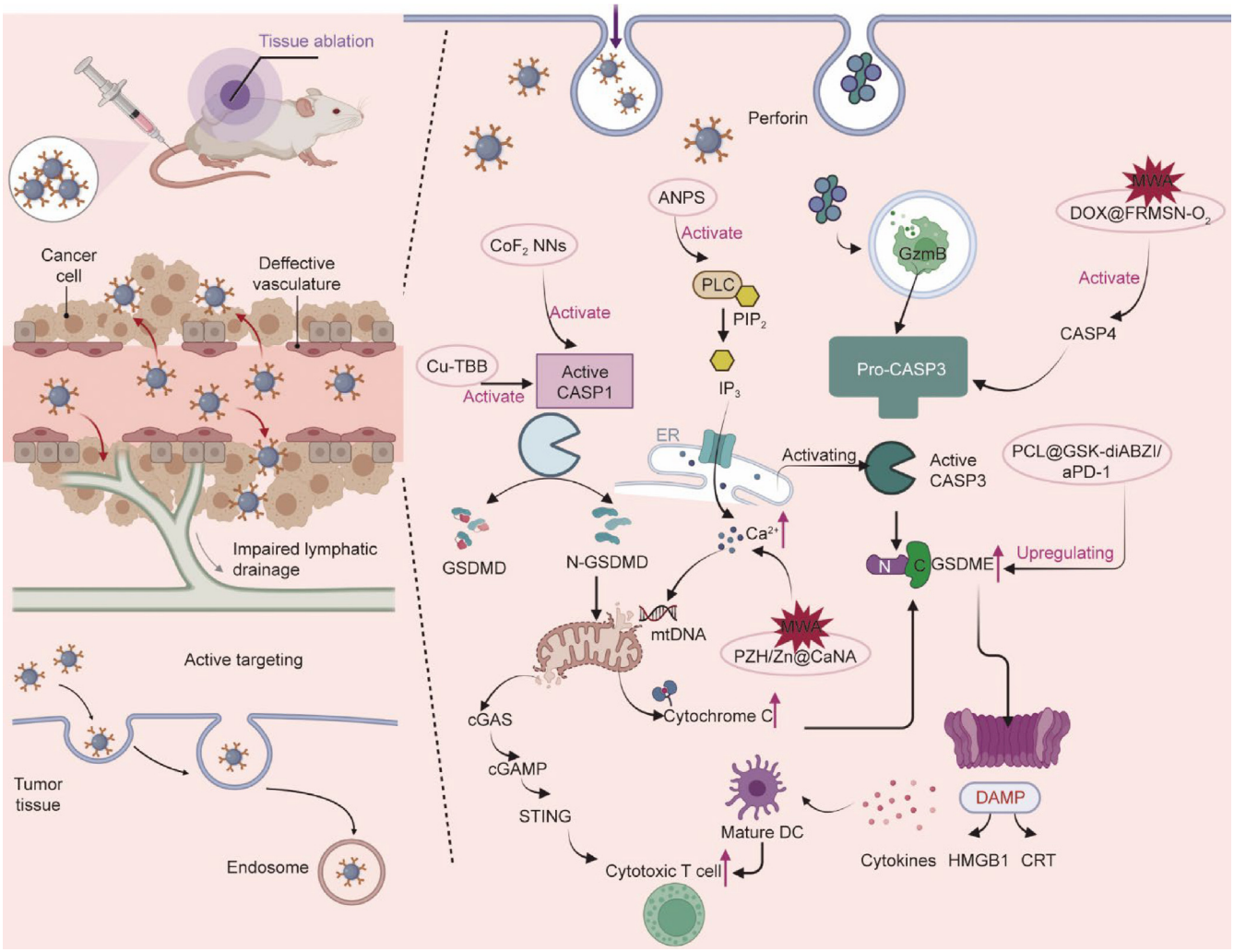

Fig. 5. Nanocarriers combine with ablation techniques to induce pyroptosis with multiple pathways. NN: nanonoodles; PLC: phospholipase C; PIP_2: phosphatidylinositol 4,5-bisphosphate; IP_3: inositol 1,4,5-trisphosphate; ER: endoplasmic reticulum; GzmB: granzyme B.

2.3.2. Nanocarrier-mediated induction of ferroptosis

Ferroptosis is a distinct form of regulated, nonapoptotic cell death that is iron-dependent and characterized by the accumulation of lipid peroxides (LPOs). Ferroptosis can be triggered by small-molecule compounds such as erastin, which disrupt intracellular redox homeostasis [147]. Morphologically, ferroptotic cells exhibit smaller mitochondria with increased membrane density and the loss of cristae while maintaining nuclear integrity—features that distinguish pyroptosis from classical apoptosis, which involves the release of cytochrome c from the mitochondria, nuclear condensation, and the formation of apoptotic bodies [148,149].

Ferroptosis inducers act directly or indirectly to inactivate glutathione peroxidase 4 (GPX4), a critical antioxidant enzyme. The inhibition of GPX4 disrupts the cellular antioxidant defense system, leading to the accumulation of ROS and LPOs, ultimately resulting in cell death [150–152]. Another key mechanism is the inhibition of the cystine/glutamate antiporter system Xc^-, which leads to GSH depletion. The resulting GSH deficiency further compromises GPX4 activity, leading to excessive lipid peroxidation that damages cellular membranes and triggers ferroptosis. LPOs are widely recognized as hallmarks of ferroptosis [152–154]. Ferroptosis is fundamentally driven by an iron-catalyzed Fenton reaction, in which intracellular ferrous ions (Fe^{2+}) facilitate the generation of lipid-based ROS. The Fe^{2+}-catalyzed conversion of lipid hydroperoxides into toxic free radicals is considered a central event in ferroptotic cell death [150,155]. Zhang et al. [156] designed a new iron supplement nanodrug (T_{10}@cLAV) by conjugating transferrin-homing peptide T_{10} on the surface of lipoic acid vesicles. This nanodrug targets transferrin in the blood to increase ferroptosis through increasing Fe^{2+} levels [156]. Zhu et al. [157] introduced Ce6-PEG-HKN15 NPs, which target ferritin to robustly activate ferroptosis. These NPs integrate the ferritin-homing peptide HKN15 with the photosensitizer chlorin e6 (Ce6) to increase ROS levels and induce ferroptosis. Feng et al. [158] introduced a microwave-activated Cu-doped zirconium metal–organic framework (CuZr MOF) as a strong microwave sensitizer. Synergistic treatment with the CuZr MOF and MWA targets GPX4 to trigger ferroptosis [158]. The synergistic nanodrug SRF@FeIIITA (SFT) was rationally designed to effectively induce ferroptosis [159]. This nanoplatform enables the intelligent, TME-responsive corelease of Fe^{2+} and sorafenib under acidic tumor conditions. Fe^{2+} catalyzes a sustained Fenton reaction, leading to the continuous generation of LPOs, while sorafenib disrupts intracellular iron homeostasis. These dual actions synergistically activate a potent ferroptotic cascade, effectively suppressing tumor proliferation. Fu et al. [160] designed an inhalable biomineralized liposome, LDM, as a ferroptosis nanoinducer. This nanoinducer conjugates

dihydroartemisinin and pH-responsive calcium phosphate to significantly increase both reactive species production and lipid peroxidation accumulation by activating endoplasmic reticulum (ER) stress [160]. Hou et al. [161] designed a nanodelivery system, red blood cell membrane (RBCM)/cyclic arginine-glycine-aspartic acid (cRGD)-modified pH-sensitive liposomes (sS@RBCM/cRGD-phLips). This system knocked out ribonucleotide reductase regulatory subunit M2 (*RRM2)* to activate the signal transducer and activator of transcription 1 (STAT1)–interferon regulatory factor 1 (IRF1)–acyl-CoA synthetase long chain family member 4 (ACSL4) axis, which can induce lipid peroxidation and ferroptosis [161]. These dual-loaded NPs present a synergistic approach that can be combined with RFA to activate ICD through the upregulation of calreticulin (CRT) and high-mobility group box 1 (HMGB1) expression.

Another study developed a DNA-free guanosine-based polymeric nanoreactor, HPG@hemin-GOx, as an inducer of both ferroptosis and apoptosis. This nanoplatform exhibits multiple enzyme-like activities, including glucose oxidase (GOx)-like, peroxidase (POD)-like, CAT-like, and GPX-like activities. Notably, the GPX-like activity of HPG@hemin-GOx leads to the depletion of intracellular GSH accompanied by the downregulation of GPX4 expression, thereby impairing the cellular antioxidant defense system. Thus, this nanoplatform promotes the excessive accumulation of LPOs and triggers ferroptosis in tumor cells [162]. Tang et al. [119] constructed a nanocarrier codelivery system that integrates cyclic arginine–glycine–aspartic acid and a RBCM, and encapsulates SPIO to specifically target fatty acid-binding protein 5. This nanocarrier can improve both RFA efficacy by increasing biocompatibility and RFA-induced ferroptosis by increasing iron levels [119] (see Fig. 6 for a schematic overview of ferroptosis pathways).

A similar mechanistic question applies to ferroptosis: What distinguishes nanocarrier-mediated ferroptosis induction from that induced by conventional small-molecule ferroptosis agents (e.g., erastin and RAS-selective lethal 3 (RSL3))? The answer again lies in the unique capabilities of nanoscale platforms.

Nanocarriers enable sustained and localized Fenton chemistry that small molecules cannot replicate. This is exemplified by the ferrous supply–regeneration nanoengine (SFT) [159]: this platform responds to the TME to codeliver Fe^{2+} and sorafenib, creating a self-amplifying cycle of lipid peroxidation. Fe^{2+} continuously catalyzes Fenton reactions, generating a sustained "ROS storm" [123] within the tumor, while sorafenib disrupts iron homeostasis. This synergistic cascade, enabled by the nanocarrier's ability to colocalize multiple agents at the tumor site, far exceeds the efficacy of either agent alone.

Nanocarriers can replenish iron and hijack endogenous iron pools through clever surface engineering. In the T_{10}@cLAV nanodrug [156], transferrin-homing peptides are conjugated to lipoic acid vesicles, effectively "hijacking" circulating transferrin to deliver iron specifically to tumor cells. This approach increases intracellular Fe^{2+} levels without the toxicity of systemic iron administration—a strategy impossible with small molecules. Similarly, Ce6-PEG-HKN15 NPs [157] target ferritin directly, redirecting the cell's own iron stores to drive ferroptosis.

The multiple enzyme-mimicking capacity of nanocarriers offers a synthetic biological approach to ferroptosis induction. The DNA-free guanosine-based polymeric nanoreactor HPG@hemin-Gox [162] simultaneously exhibits GOx-like, POD-like, CAT-like, and GPX-like activities. This "all-in-one" enzymatic platform depletes glutathione, downregulates GPX4, and promotes lipid peroxidation through a coordinated cascade—an extent of multifunctionality unattainable with simple small-molecule inhibitors.

2.3.3. Crosstalk and context-dependency of pyroptosis and ferroptosis in the ablation milieu

While pyroptosis and ferroptosis are often discussed as distinct, parallel pathways, emerging evidence suggests significant crosstalk and context-dependent interplay between them, particularly within the unique stress milieu of an ablation zone. Understanding this interplay is critical for the rational design of nanocarrier combinations.

Both pathways can be triggered by common upstream events relevant to ablation, such as oxidative stress and mitochondrial dysfunction. ROS generated by thermal stress or the Fenton reaction can simultaneously activate inflammasome complexes (leading to pyroptosis) and promote lipid peroxidation (leading to ferroptosis) [123,133]. This convergence suggests that nanocarriers designed to amplify oxidative damage may inadvertently activate both pathways, potentially increasing overall immunogenicity.

Iron metabolism, which is central to ferroptosis, also influences pyroptotic signaling. Excess intracellular iron can catalyze ROS production, which in turn can activate the NOD-like receptor family pyrin domain-containing protein 3 (NLRP3) inflammasome [150]. Conversely, robust inflammatory cytokine release (IL-1β and IL-18), which is characteristic of pyroptosis [134,136], can upregulate hepcidin expression and alter systemic iron distribution, potentially creating a microenvironment that is more conducive to ferroptosis. The dominant cell death pathway may shift depending on the localization relative to the ablation center and the temporal phase postablation. In the central coagulation zone during thermal ablation, immediate necrosis is predominant, but surviving cells at the peripheral margin experience sublethal stress [48,49]. Here, hypoxia and iron accumulation may favor ferroptosis [163]. In the inflammatory recovery phase, DAMPs released from dying cells [138,164] may prime the innate immune system, potentially lowering the threshold for pyroptosis induction in infiltrating immune cells or residual tumor cells.

This crosstalk presents both opportunities and challenges. Nanocarriers could be engineered to target both pathways in a "belt-and-suspenders" approach to tumor eradication. For example, a nanoplatform combining iron delivery (for ferroptosis induction) with STING activation could leverage the synergy between these pathways. This context dependency indicates that the optimal strategy may vary by tumor type, ablation modality, and nanocarrier administration timing. Future studies should systematically investigate this interplay using spatially resolved profiling of the ablation zone.

2.4. Nanocarriers in tumor diagnosis

Early detection and accurate diagnosis of malignant tumors are vital for improving patient survival [165,166]. Currently, tumor monitoring relies primarily on biomarker detection and imaging. Early-stage tumors are often detected on the basis of circulating biomarkers; however, most tumor-derived biomarkers are shed from tumor tissues and become highly diluted in the bloodstream, leading to low specificity and limited diagnostic accuracy [167]. Imaging modalities, such as CT and MRI, are also widely used for tumor diagnosis, but they often lack sufficient sensitivity to detect tumors at an early stage [168,169].

Nanocarriers have attracted widespread attention because of their broad applications in cancer diagnosis, immunoassays, genetic research, and bioseparation, ultimately contributing to improving public health [170,171]. Owing to their unique physical and chemical properties, gold NPs have been widely employed in the development of biosensing platforms. Their advantages include accelerated signal transduction, increased signal intensity, and a straightforward signal readout, making them highly suitable for biochemical analyses [119,172].

Keliher et al. [173] developed a macrophage-specific PET imaging agent composed of ^{89}Zr-labeled cross-linked short-chain dextran NPs that enabled quantitative assessment of inflammation levels and holds great potential for diagnosing and treating

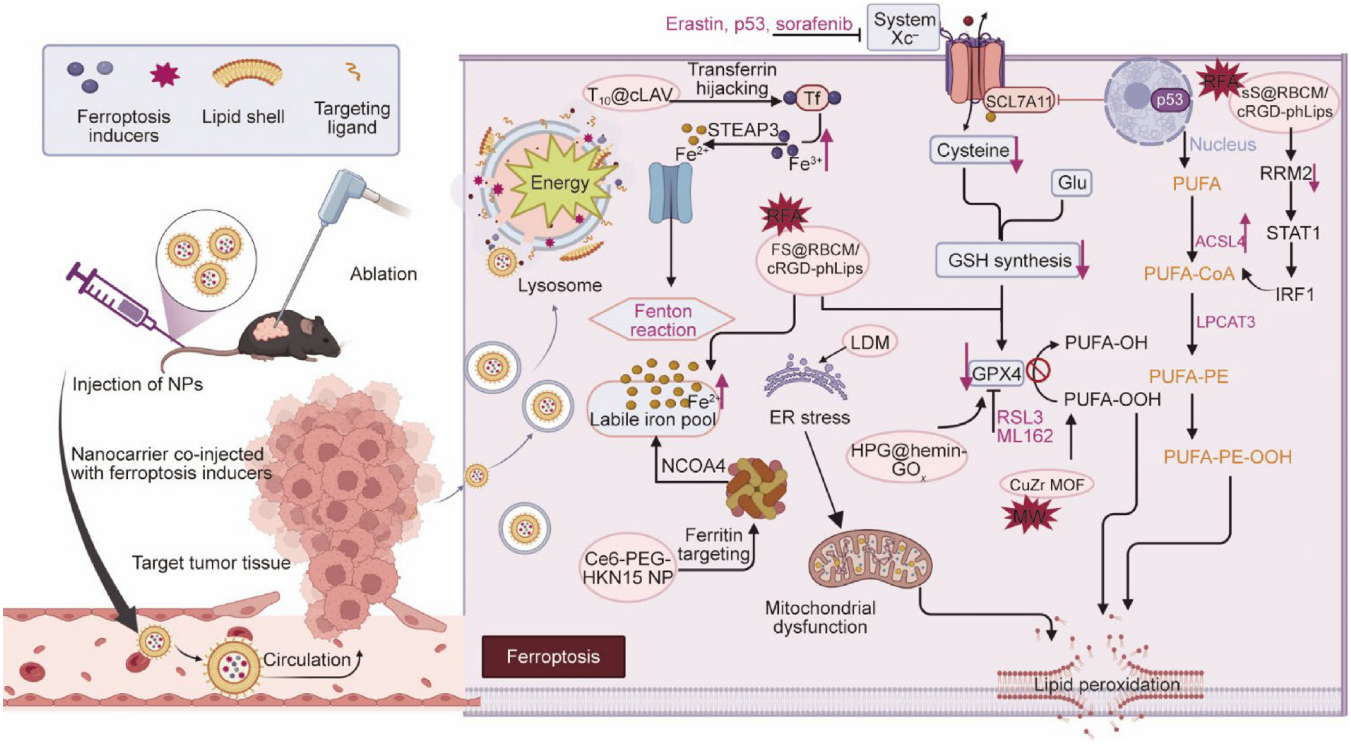

Fig. 6. Nanocarriers combine with ablation techniques to trigger ferroptosis with multiple pathways. NCOA4: nuclear receptor coactivator 4; STEAP3: six-transmembrane epithelial antigen of prostate 3; SCL7A11: solute carrier family 7 member 11; PUFA: polyunsaturated fatty acid; RSL3: RAS-selective lethal 3; CoA: coenzyme A; LPCAT3: lysophosphatidylcholine acyltransferase 3; PE: phosphatidylethanolamine.

inflammation-associated cancers. In addition, emerging platforms such as MOFs have shown promise in ablation combination diagnosis. MOFs are hybrid materials composed of metal ions or clusters coordinated to organic linkers that are characterized by high porosity, tunable structures, and biodegradability [174]. The key characteristics of the different nanocarrier platforms discussed in this section are summarized in Table 2 [65,66,68,70,71,73,75, 77, 79,110,118,119,129,158,172,174–176], which provides a comparative overview of their core materials, main characteristics, and clinical translation status.

3. Comparative analysis of post-ablation microenvironments

While the various cell death pathways activated by nanocarriers were detailed in the previous sections, the efficiency of the induction of these pathways is profoundly influenced by the specific TME remodeled by different ablation techniques. A critical consideration for designing effective combination strategies is the recognition that thermal ablation (RFA/MWA) and nonthermal ablation (IRE/Cryo) leave fundamentally different biological landscapes behind.

Thermal ablation (RFA and MWA), despite its potent local tumor destruction capability, often induces a state of acute hypoxia in the peripheral ablation zone because of microvascular disruption and coagulation necrosis [177,178]. This hypoxic niche not only promotes the survival of residual tumor cells but also serves as a recruitment signal for immunosuppressive cells such as MDSCs and Tregs, resulting in a profoundly iTME [179,180]. Consequently, nanocarriers designed to synergize with RFA/MWA must prioritize hypoxia relief (e.g., oxygen-carrying NPs [129,146]), immunosuppressive metabolism reprogramming (e.g., cholesterol-targeting hydrogels [62]), and the induction of ferroptosis, which thrives in such oxidative and iron-rich environments [119,158,161].

In stark contrast, nonthermal ablation techniques, particularly IRE and Cryo, preserve the integrity of the ECM and major blood vessels [40,181]. Such preservation of the vasculature minimizes the degree of postablation ischemia and hypoxia. Instead, these modalities are characterized by the rapid and robust release of DAMPs, such as adenosine triphosphate (ATP) and HMGB1, which potently activate DCs and prime adaptive immunity [1648,182]. Therefore, the mechanistic requirements for nanocarriers are different in this context. The emphasis is less on alleviating hypoxia and more on amplifying ICD signals, capturing and presenting tumor antigens (as with nanovaccines [97]) and inducing long-term "trained immunity" in peripheral immune organs such as the spleen [183].

In the following sections, we detail how nanocarriers fulfill key functional roles when applied in combination with ablation therapies.

4. Integration of nanocarriers with tumor ablation therapies

4.1. Core mechanisms of synergy between nanocarriers and ablation therapies

Before discussing modality-specific applications, it is important to recognize the core mechanisms that underlie the synergy between nanocarriers and various ablation techniques. These common principles form the theoretical foundation for the analysis of nanocarrier applications with specific ablation modalities in the following sections.

Thermal ablation techniques (RFA and MWA) often exacerbate tumor hypoxia, which promotes immunosuppression and treatment resistance, whereas nanocarriers equipped with oxygen-carrying or oxygen-generating capabilities can alleviate this hypoxic microenvironment, promoting both direct cell death and immune activation [93,127,145]. Although ablation triggers the

Table 2
Summary of the main characteristics of nanocarriers.

Type of nanocarrier	Core materials	Main Characteristics	Refs.
Liposome	Phospholipids, cholesterol	Optimal biocompatibility; analogous to cell membrane structure; can load both hydrophilic and lipophilic drugs; among the earliest in clinical translation	[70,71,73]
Polymeric micelle	Amphiphilic block copolymers	Small nanoscale size (10–100 nm); facilitates tumor penetration; hydrophobic core efficiently encapsulates insoluble drugs; hydrophilic shell prolongs circulation time	[65,66,68]
Dendrimer	Highly branched synthetic macromolecules	Precisely controllable structure; abundant surface functional groups for easy modification; internal cavities can carry drugs	[66,68]
Inorganic NP	Gold NPs: gold; magnetic NPs: iron oxide; MOFs: metal ions/clusters^{+}; organic linkers; mesoporous silica: silicon dioxide	Gold: PTT, CT imaging; magnetic NPs: MRI imaging, magnetic hyperthermia, magnetic targeting; high porosity; tunable structure; biodegradable; microwave sensitizing capability; mesoporous silica: high drug loading capacity, easy functionalization	[172,175110,119158,174,176118,129]
Albumin NP	Human serum albumin	High biosafety; no need for synthetic materials; penetrates vasculature via GP60 receptor-mediated transport	[75]
Nucleic acid nanocarrier	DNA or RNA molecules	Self-assembly via base pairing; programmable structure; precise size and shape; biodegradable; good biocompatibility	[77,79]

release of DAMPs, this effect is often transient; nanocarriers coloaded with ICD inducers (e.g., chemotherapeutics and photosensitizers) can amplify DAMP release, promoting DC maturation and T-cell priming [126,183,184]. Furthermore, the post-ablation TME is frequently characterized by immunosuppression featuring MDSCs infiltration and M2 macrophage polarization; nanocarriers designed to deliver immunomodulators (e.g., STING agonists and checkpoint inhibitors) can reprogram this landscape toward an antitumor phenotype [110,117,185].

Beyond apoptosis, nanocarriers can trigger ICD pathways such as ferroptosis and pyroptosis, which release proinflammatory signals and enhance systemic antitumor immunity [110,119,138,157]. Moreover, stimuli-responsive nanocarriers (thermosensitive, pH-sensitive, and enzyme-responsive) enable targeted drug delivery to the ablation zone, maximizing local efficacy while minimizing systemic toxicity [73,128,158]. These mechanisms do not operate in isolation but rather synergize with one another; for example, hypoxia relief can promote the induction of ICD, while ICD can further remodel the TME, creating a positive feedback loop. Understanding these core mechanisms and their interplay is essential for rationally designing nanocarrier strategies tailored to different ablation modalities. The following sections build upon these common principles, emphasizing the mechanisms most relevant to each ablation technique.

4.2. Nanocarrier-enhanced RFA

RFA induces coagulative necrosis in tumor tissues by causing localized thermal injury [37,186,187]. Beyond its direct physical cytotoxicity, RFA can enhance tumor immunogenicity through the release of endogenous DAMPs that activate DCs. Evidence suggests that RFA-induced tumor damage promotes antigen presentation, increases T-cell infiltration, and triggers tumor-specific immune responses, particularly in patients with HCC [188–190]. RFA-induced thermal stress also stimulates the activation and phenotypic maturation of NK cells and facilitates the generation of tumor antigen-specific $CD4^{+}$ and $CD8^{+}$ T cells, as well as tumor-specific antibodies, thereby enhancing systemic antitumor immunity [163,191,192].

However, compared with surgical resection, RFA monotherapy is associated with a significantly higher recurrence rate [193]. The immunostimulatory effects of RFA are often transient and insufficient to elicit durable tumor-specific T cell memory responses. Clinical observations have revealed that the abundance of tumor-associated antigen (TAA)-specific T cells gradually decreases within 24 weeks after RFA and that their memory phenotype and longevity are inadequate to prevent tumor relapse and metastasis, particularly in patients with HCC [194]. In addition, incomplete ablation and localized thermal injury can exacerbate tumor hypoxia, leading to the formation of an immunosuppressive tumor microenvironment (ITM), which not only reduces the efficacy of RFA-induced immune responses but also may facilitate tumor progression and distant metastasis [177,178,195].

The rationally designed nano-epidrug MFMP was developed to simultaneously mediate DNA and RNA demethylation, thereby reactivating silenced immune pathways. When combined with insufficient radiofrequency ablation (iRFA), MFMP significantly promoted ICD and increased TAA release. This combination therapy synergistically enhanced T-cell effector function, leading to a 3.2-fold increase in tumor-infiltrating $CD8^{+}$ T cells and a 60% reduction in PD-L1 expression while inducing robust immune memory that suppressed tumor growth by 85% and significantly reduced metastasis in HCC models [118].

Biomimetic nanovesicles coated with immune cell-derived membranes have demonstrated marked effects, including prolonging systemic circulation, improving antigen-specific targeting, sustaining drug release, and reducing systemic toxicity [196,197]. These features make biomimetic nanovesicles ideal carriers for cancer immunotherapy, particularly in combination with local ablation techniques such as RFA.

A recent study developed a novel biomimetic nanoplatform, PML@Len, by cloaking NPs with macrophage membranes overexpressing programmed cell death protein-1 (PD-1), which enables targeting to residual tumor tissue after RFA, remodels the ITM, and prevents tumor recurrence. Compared with RFA alone, PML@Len exhibited excellent structural stability and drug loading efficiency, enabling targeted delivery to residual tumor tissue after RFA, which reduced recurrence rates by 70% (from 65% to 19%) and extended the median survival from 38 to 62 days [198]. This was accompanied by a 4.5-fold increase in the number of tumor-infiltrating $CD8^{+}$ T cells and a 55% reduction in the number of Tregs.

This targeted delivery system significantly increases local immunomodulation and promotes tumor-specific immune responses. Tang et al. [119] designed a novel nanocarrier codelivery system to amplify ferroptosis and reprogram the TME. The pro-

posed nanocarrier integrates cRGD and a RBCM and encapsulates SPIO to specifically target fatty acid-binding protein 5 in tumor cells. These findings demonstrate that nanocarriers exert antitumor effects primarily through the activation of ferroptosis. Additionally, the impact of immunotherapy is underscored by the increased antitumor immune responses characterized by increased infiltration of cytotoxic T cells and inflammatory cytokines. The nanocarrier codelivery system increased RFA efficacy, resulting in tumor volume inhibition of 92% and a complete ablation rate of 75%, accompanied by a 5.2-fold increase in CTL infiltration and a 3.8-fold increase in the number of interferon-γ (IFN-γ)$^+$CD8$^+$ T cells [119] (see Fig. 7 for experimental validation).

4.3. Nanocarrier-enhanced MWA

MWA is a minimally invasive technique that induces localized tumor necrosis via high-frequency electromagnetic heating [37]. MWA is not only a local tumor-eradicating modality but also an immune-activating intervention that contributes to long-term antitumor responses. After ablation, MWA can activate macrophages, which release proinflammatory cytokines such as IL-15, thereby increasing NK cell cytotoxicity and the CTL/Treg ratio, and promoting CD8$^+$ T cell cytotoxicity, leading to durable systemic antitumor immunity, metastasis inhibition, and improved overall survival [199,200]. In patients with HCC, MWA has been reported to enhance tumor-specific immune reactions, potentially inducing an abscopal effect to suppress the growth of untreated distant lesions [195,201].

MWA can also trigger the release of DAMPs, activate the inducible T-cell co-stimulator (ICOS) pathway, recruit immune cells, and initiate CD4$^+$ T cell memory formation and T helper 1-type immune responses. This cascade leads to tumor antigen-specific systemic immunity [202–204].

Despite these immunological benefits, MWA is hampered by a high postoperative recurrence rate [205]. Owing to the irregular morphology of most tumors, larger ablation volumes are often required to achieve complete tumor eradication, which may result in collateral thermal injury to adjacent healthy tissues and increase the risk of adverse effects [206,207]. In addition, only some patients derive meaningful clinical benefit, likely because of interindividual variability in immune responses, and MWA has only a moderate effect on circulating immune cell subsets [201,203,208].

Combining MWA with immune checkpoint inhibitors (ICIs) has shown promise in increasing ICI efficacy [207,209]. However, the overall clinical response rate remains limited, with only 15%–20% of patients showing objective benefit [185,210]. To address these limitations, a novel metal–alginate hydrogel coloaded with Mn^{2+} and Ca^{2+} was developed as a microwave sensitizer. This hydrogel increased MWA efficacy at lower power settings, achieving a 2.3-fold larger ablation zone and 60% complete response rate, with a 4.8-fold increase in STING pathway activation and a 5.2-fold increase in IFN-β levels [63].

Crucially, Mn^{2+} released from the hydrogel activates the STING pathway, whereas Ca^{2+} influx induces oxidative stress and mitochondrial dysfunction, efficiently triggering ICD. The resulting release of DAMPs further activates both innate and adaptive immunity, ultimately suppressing tumor recurrence and metastasis while establishing long-term immune memory. To address MWA-induced hypoxia, Guo et al. [211] developed GaMOF-Arg-TPP (GAT) microwave (MW) immunosensitizers that release NO under microwave irradiation. NO downregulates hypoxia-inducible factor-1α (HIF-1α) to alleviate hypoxia, induces mitochondrial damage to increase thermal sensitivity, and increases CRT exposure, HMGB1 release, and T-cell proliferation to trigger ICD. In a 4T1 model, GAT MW achieved 100% tumor inhibition, increased the percentage of intratumoral CD8$^+$ T cells from 16.8% to 33.2%, and effectively inhibited lung metastasis [211].

In addition, cholesterol metabolism within the TME has emerged as a key barrier to effective immunotherapy. Cholesterol-derived metabolites promote tumor progression by inducing immune checkpoint expression and CD8$^+$ T cell exhaustion. This cholesterol-driven immunometabolism significantly compromises the synergy between MWA and ICIs [212–214]. To overcome this issue, a new cholesterol-targeting catalytic hydrogel, DA-COD-OD-HCS, was engineered, that combines microwave sensitivity and immunostimulatory properties, to potentiate the therapeutic synergy between MWA and ICIs in the context of HCC [62]. In the acidic, residual ITM formed after MWA, the hydrogel enables sustained, stable release of cholesterol oxidase (COD), which efficiently degrades cholesterol fragments. DA-COD-OD-HCS responded to the post-MWA microenvironment in orthotopic HCC models, continuously releasing COD and inducing ferroptosis in tumor cells, thereby amplifying antitumor immunity. When combined with anti-PD-L1 immunotherapy, this platform inhibited primary tumor growth by 88% and reduced distant metastasis by 90%, with a 6.1-fold increase in the number of tumor-infiltrating CD8$^+$ T cells and a 4.3-fold increase in the number of tumor necrosis factor-α (TNF-α)$^+$CD8$^+$ T cells, effectively preventing HCC recurrence (see Fig. 8 for characterization and efficacy data). Wu et al. [174] engineered MnCa-MOF nanoactivator (MPPT NAs) coloaded with pyrotinib and a PD-1/PD-L1 inhibitor. Under microwave irradiation, ROS are generated for dynamic MWA therapy, promoting DC maturation and CTL infiltration. This strategy resulted in 98.7% primary tumor inhibition, significantly suppressed distal tumors and lung metastases, and increased CD8$^+$ T cell infiltration [174]. Li et al. [176] engineered a bismuth-based MOF (BMCPH) that functions as both a microwave sensitizer and an H_2S immunomodulator. Under microwave irradiation, H_2S is released via cystathionine-β-synthase (CBS) that is overexpressed on tumor cells, inhibiting MDSCs and promoting CTL infiltration, while the Bi-MOF core scavenges ROS to dampen immunosuppression. This strategy increased the number of intratumoral CD8$^+$ T cells by 6-fold, reduced lung metastases, and achieved long-term tumor suppression [176]. In addition, Wang et al. [146] engineered a protein corona-detachable MWA amplifier (DOX@FRMSN-O_2). Upon microwave irradiation, O_2 bubbles release strips of the adsorbed protein corona via inertial cavitation, increasing intratumoral accumulation, whereas oxygenation reverses hypoxia and promotes vascular normalization. These amplifiers activate the noncanonical pyroptosis pathway via CASP4/GSDME cleavage, repolarizing cancer cells into senescent cells. In a HCC model, this strategy extended the median survival beyond 40 days (vs < 20 days) [146].

Nanoplatforms have emerged as powerful tools in this context because of their ability to increase therapeutic efficacy, minimize side effects, provide precise spatiotemporal control, improve imaging-guided interventions, and synergize with other therapeutic strategies for comprehensive tumor eradication [215].

4.4. Nanocarrier-enhanced PDT/PTT

Phototherapy, including PDT and PTT, is a noninvasive modality that uses light to precisely eliminate cancer cells by generating ROS or inducing localized hyperthermia [216,217]. Temperatures above 40–43 °C can lead to cell membrane disruption, protein denaturation, and tumor tissue ablation [60]. Both PDT and PTT exert direct toxic effects on tumor cells by producing singlet oxygen or elevating the tissue temperature. They can also damage the tumor vasculature and induce localized inflammation, thereby increasing vascular permeability and remodeling the ECM. These effects enhance the EPR effect, allowing for passive tumor targeting and improved intratumoral drug delivery [218,219]. Because of

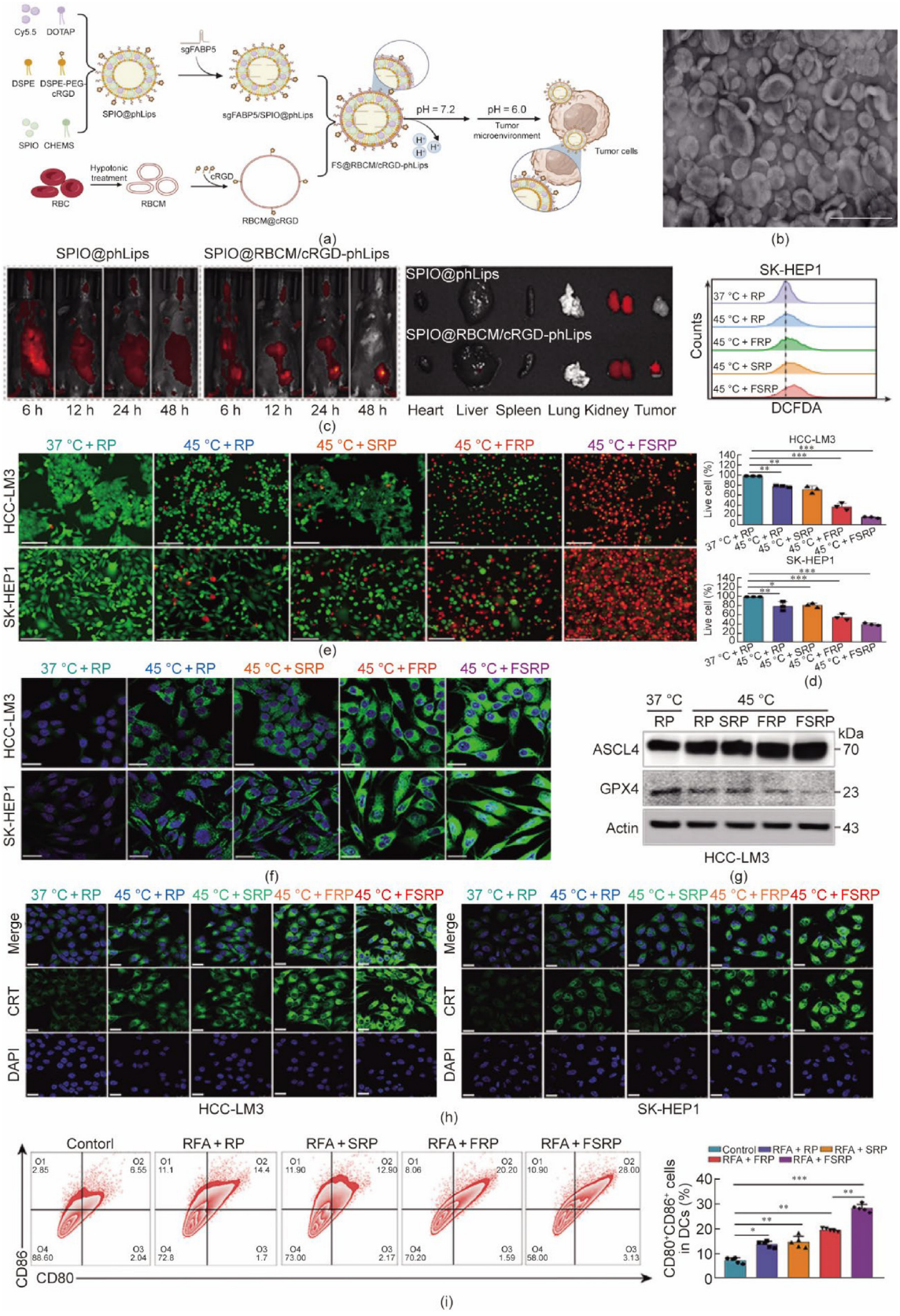
Cy5.5
DOTAP
DSPE
DSPE-PEG-cRGD
SPIO
CHEMS
SPIO@phLips
sgFABP5
sgFABP5/SPIO@phLips
FS@RBCM/cRGD-phLips
pH = 7.2
pH = 6.0
Tumor microenvironment
Tumor cells
RBC
Hypotonic treatment
RBCM
cRGD
RBCM@cRGD
(a)
(b)
SPIO@phLips
SPIO@RBCM/cRGD-phLips
6 h
12 h
24 h
48 h
Heart
Liver
Spleen
Lung
Kidney
Tumor
(c)
SK-HEP1
37 °C + RP
45 °C + RP
45 °C + FRP
45 °C + SRP
45 °C + FSRP
Counts
DCFDA
37 °C + RP
45 °C + RP
45 °C + SRP
45 °C + FRP
45 °C + FSRP
HCC-LM3
SK-HEP1
(e)
HCC-LM3
SK-HEP1
Live cell (%)
(d)
37 °C
45 °C
RP
SRP
FRP
FSRP
kDa
ASCL4
GPX4
Actin
70
23
43
HCC-LM3
(g)
Merge
CRT
DAPI
HCC-LM3
SK-HEP1
(h)
Contorl
RFA + RP
RFA + SRP
RFA + FRP
RFA + FSRP
CD86
CD80
CD80+CD86+ cells in DCs (%)
(i)

minimal collateral damage and a negligible increase in temperature in the surrounding healthy tissues, PDT is particularly suitable for treating cutaneous malignancies and has shown excellent cosmetic outcomes [61].

In solid tumors, hypoxia, which is caused mainly by rapid and abnormal tumor cell proliferation, leads to the overexpression of hypoxia-inducible factors, which are associated with radioresistance, chemoresistance, increased invasiveness, and metastatic potential [220]. Beyond direct tumor cell ablation, PDT and PTT also effectively induce ICD and have potent immune-activating effects [127]. Nanocarriers with broad-spectrum photonic absorption exhibit unique optical properties that enable light to penetrate deep into tissue, allowing effective tumor ablation even in deep-seated lesions [184].

Given that most patients with cancer are diagnosed at an advanced stage with a high tumor burden, prognosis and therapeutic efficacy are often compromised. To address this challenge, one study designed a self-assembled nanoassembly (NA) composed of Ce6 and mitoxantrone, termed CM NAs [221]. Upon a single exposure to 660 nm laser irradiation, CM NAs synergistically enhanced the effects of both PTT and PDT in large tumors, reducing tumor volume by 94% and achieving 50% complete regression, with a 3.5-fold increase in CRT exposure and a 4.1-fold increase in HMGB1 release, indicating robust ICD. CM NAs exhibit favorable biocompatibility, low toxicity in the absence of irradiation, minimal phototoxicity, and selective accumulation in tumors without affecting healthy tissues or organs.

Another study developed the nanoplatform FPc NPs based on phthalocyanine (Pc)-polymerized Pluronic NPs, which demonstrated increased cancer cell targeting [222]. Upon continuous near-infrared irradiation, compared with individual Pc dyes or simple aggregates, FPc NPs exhibited superior photothermal effects, effectively inducing tumor cell death.

Another study developed a multifunctional nanodrug, SFT, for a combination therapy by combining ferroptosis induction with photodynamic therapy [159]. This nanodrug incorporates methylene blue as a photosensitizer for tumor imaging and light-triggered therapy. The iron-replenishing component promotes ferroptosis, further enhancing tumor suppression, inducing long-term cytotoxicity, and significantly inhibiting tumor proliferation. This dual-modal approach not only improves tumor-killing efficiency but also offers precise spatial control over the therapeutic process, highlighting its potential as a powerful theranostic platform for precision oncology.

4.5. Nanocarrier-enhanced IRE

IRE is a nonthermal local ablative technique that eradicates tumor tissue by applying short, high-voltage electric pulses that disrupt cell membrane integrity and induce a permanent loss of homeostasis, leading to cell death [59]. Unlike thermal ablation, IRE preserves critical structures such as blood vessels, nerves, and adjacent organs, minimizing collateral damage [37,181,223,224]. For instance, in the treatment of localized prostate cancer, percutaneous IRE effectively ablated tumor tissue while exerting minimal effects on the rectum, urethra, and neurovascular bundles [225].

Beyond direct cytotoxicity, IRE can also trigger ICD, characterized by the release of DAMPs such as CRT, ATP, and HMGB1 [164,226]. Extracellular ATP serves as a potent signal that activates DCs, promoting IL-1β secretion and initiating $CD8^+$ T cell-mediated cytotoxic responses [182]. After release due to electroporation-induced stress or ionizing radiation, HMGB1 binds to toll-like receptor 4 on DCs, enhancing antigen presentation and CTL activation [227–230].

In a rat osteosarcoma model, IRE treatment significantly increased the numbers of cluster of $CD3^+$ and $CD4^+$ T cells, as well as the $CD4^+/CD8^+$ ratio, within seven days post-ablation, indicating a stronger cellular immune response to IRE compared to surgical resection [231,232]. These findings suggest that IRE can induce robust ICD and enhance antitumor immunity.

As hematopoietic organs rich in myeloid cells, the spleen and bone marrow can be exploited to modulate trained immunity via LNP delivery systems. Myeloid cells exhibit heightened antigen responsiveness following activation by DAMPs or pathogens [233–235]. Targeting the spleen has emerged as a promising strategy to elicit potent systemic immune responses against tumors. Precise modulation of splenic and myeloid cell subsets may unlock the full therapeutic potential of trained immunity and increase antitumor immune efficacy.

One study developed a nanobiotherapeutic formulation, MDCa@RBC-Alipo, to enhance IRE-induced immune responses in patients with advanced and unresectable pancreatic cancer by inducing trained immunity [183]. In conjunction with phospholipids, other lipids, and apolipoprotein A1 (APOA1), this nanoplatform preferentially accumulated in the spleen and modulated myeloid cells via epigenetic and metabolic reprogramming. By activating splenic myeloid cells, MDCa@RBC-Alipo enhanced peripheral trained immune responses by 320%, extended median survival from 41 to 68 days, and reduced metastasis by 85% when combined with IRE and anti-PD-L1 therapy (see Fig. 9 for synthesis and biodistribution data).

Another study developed a multifunctional nanoplatform, M-TK-OA, for the codelivery of two DNA repair inhibitors, olaparib and AZD0156, to impair the DNA damage repair machinery in pancreatic cancer cells [236]. When combined with IRE, M-TK-OA prolonged the median survival from 41 to 68 days, with 40% of the mice achieving long-term survival (>90 days) compared with 0 after treatment with IRE alone, accompanied by a 4.2-fold increase in the number of tumor-infiltrating $CD8^+$ T cells and a 3.1-fold increase in the number of central memory T cells. Importantly, the loading of multiple therapeutic agents into a single nanocarrier enables efficient, synergistic combination therapy, which is crucial for treating aggressive, immune-evasive tumors such as pancreatic tumors. The combination

Fig. 7. Nanocarriers enhance tumor sensitivity to RFA and antitumor immunity, thereby achieving synergistic therapeutic effects. (a) Schematic diagram depicting the structural modifications of LNPs. (b) Representative transmission electron microscopy (TEM) images displaying the morphology of the modified LNPs. Scale bar = 100 nm. (c) Fluorescence imaging of *in vivo* and *ex vivo* distributions of NPs in organs and tumors. (d) Flow cytometric analysis of ROS levels in SK-HEP-1 cells across five treatment groups, measured by dichlorofluorescein diacetate (DCFDA) fluorescence intensity, with the 37 °C + @RBCM/cRGD-phLips (RP) group serving as the control. (e) Viability of HCC-LM3 and SK-HEP-1 cells under five treatment conditions using calcein acetoxymethyl ester (AM; green, viable cells) and ethidium homodimer-1 (Eth-1; red, non-viable cells) double staining. Scale bars = 100 μm. (f) Representative immunofluorescence images showing BODIPY-C11 staining of HCC-LM3 and SK-HEP1 cells under the specified treatments. Scale bars = 100 μm. (g) Western blot analysis examining acyl-CoA synthetase long chain family member 4 (ASCL4) and GPX4 expression levels in HCC-LM3 and SK-HEP-1 cells under the indicated treatments. (h) Representative immunofluorescence images depicting CRT expression under different treatment conditions. Scale bars = 100 μm. (i) Flow cytometry false-color plots depicting CD80 and CD86 expression in live-cell gated HCC tumor tissues, with histograms showing the percentage of $CD80^+CD86^+$ DCs. DSPE: 1,2-distearoyl-sn-glycero-3-phosphoethanolamine; DOTAP: 1,2-dioleoyl-3-trimethylammonium-propane; PEG: polyethylene glycol; CHEMS: cholesteryl hemisuccinate; FABP5: fatty acid binding protein 5; FRP: sgFABP5@RBCM/cRGD-phLips; SRP: SPIO@RBCM/cRGD-phLips; FSRP: FS@RBCM/cRGD-phLips; DAPI: 4',6-diamidino-2-phenylindole. Reproduced from Ref [119] with permission.

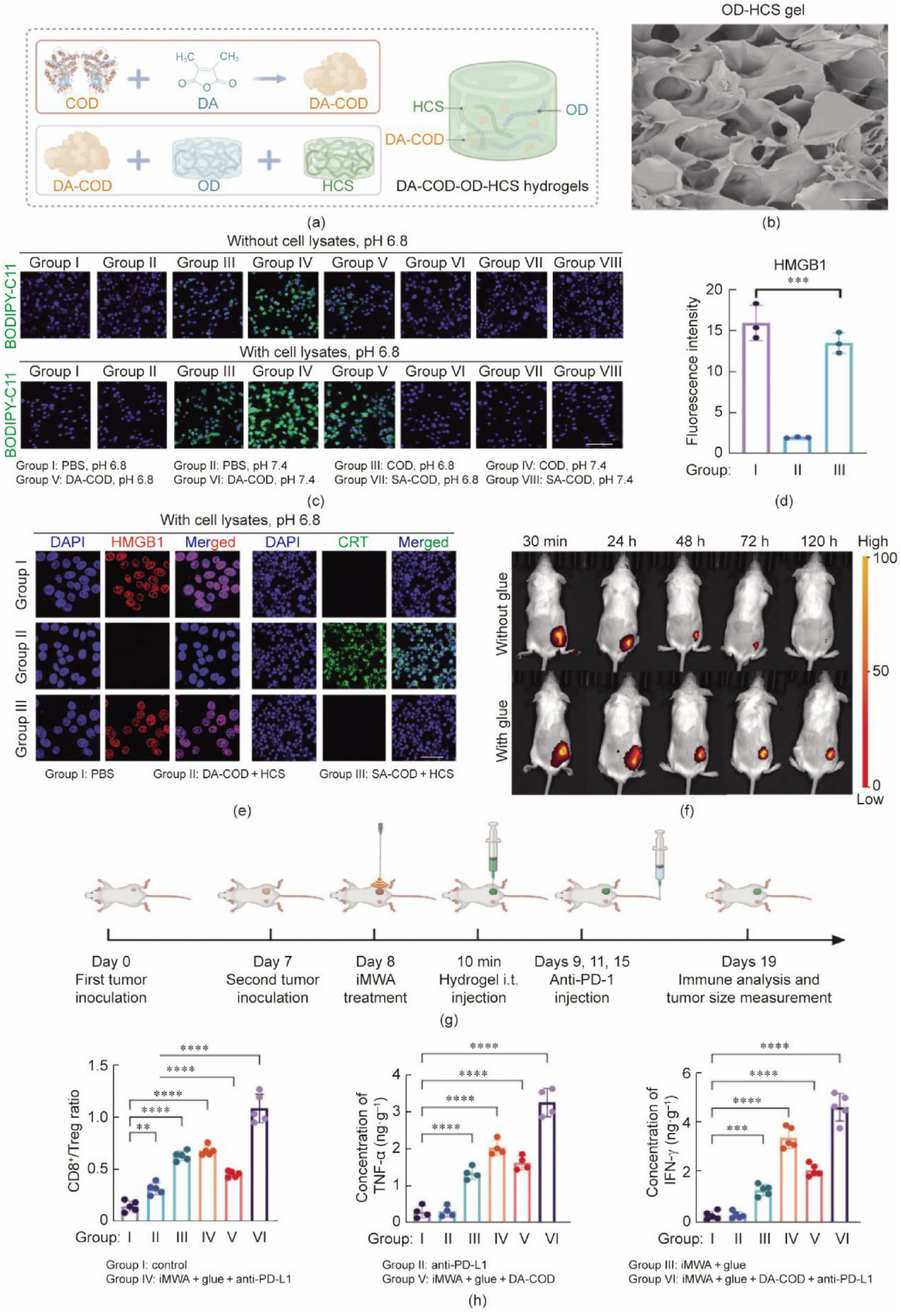

Fig. 8. Nanocarriers enhance tumor sensitivity to MWA and antitumor immunity, thereby achieving synergistic therapeutic effects. (a) Schematic illustration of the synthesis process of dimethylmaleic anhydride (DA)-cholesterol oxidase (COD)-oxidized dextran (OD)-hemin-chitosan (HCS) hydrogels. (b) Scanning electron microscopy (SEM) image of the OD-HCS hydrogel. Scale bar = 200 μm. (c) Confocal imaging of the intracellular lipid peroxidation of H22 cells subjected to different treatments, as indicated, in the absence or presence of cell lysates stained with the BODIPY-C11 probe. Scale bar = 20 μm. (d) Intracellular ferroptosis of fluorescence intensity in H22 cells after various treatments, as indicated. (e) Confocal images of intracellular ferroptosis in H22 cells after various treatments, as indicated. Scale bar = 20 μm. (f) *In vivo* fluorescence imaging of H22 tumor-bearing mice intratumorally injected with Cy5.5-labeled DA-COD in the presence or absence of OD-HCS adhesive glue at the indicated time points post incomplete microwave ablation (iMWA) treatment. (g) A schematic illustration of the inoculation of the bilateral tumor model for *in vivo* antitumor and immune mechanism studies. (h) Flow cytometry statistical histograms showing the frequencies of $CD8^+$ T cells in distant tumors after various treatments. The TNF-α and IFN-γ secretion levels in distant tumors after various treatments. Glue: OD-HCS hydrogels; SA: succinic anhydride; i.t.: intratumoral. Reproduced from Ref [62] with permission.

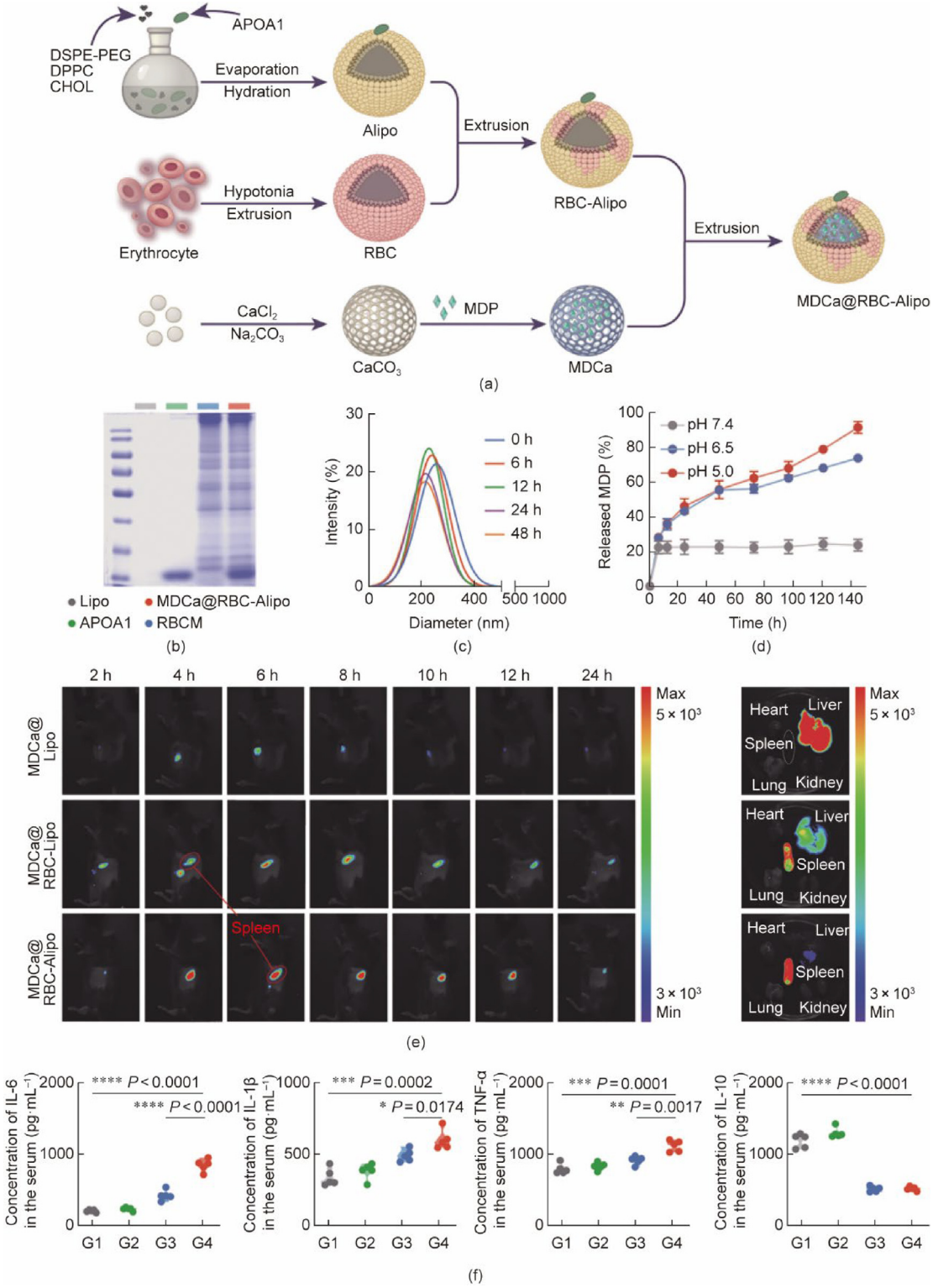

Fig. 9. Nanocarriers enhance tumor sensitivity to IRE and antitumor immunity, thereby achieving synergistic therapeutic effects. (a) A scheme indicating the step-by-step synthesis of MDCa@RBC-Alipo. (b) Sodium dodecyl sulfate polyacrylamide gel electrophoresis (SDS–PAGE) pattern of proteins from liposome, APOA1, red blood cell membrane, and MDCa@RBC-Alipo lysates. (c) Size changes of MDCa@RBC-Alipo NPs in phosphate buffer saline (PBS) to prove stability. (d) Cumulative release profiles of muramyl dipeptide (MDP) from $CaCO_3$ in solutions at different pH values. Data were presented as means ± SD (n = 3). (e) Fluorescence images to reveal the biodistribution of MDCa@Lipo, MDCa@RBC-Lipo, or MDCa@RBC-Alipo post intravenous (i.v.) injection at the indicated time points. Fluorescence imaging of dissected organs 6 h after intravenous injection of MDCa@Lipo, MDCa@RBC-Lipo, or MDCa@RBC-Alipo. (f) Cytokine levels of IL-6, IL-1, TNF-α, and IL-10 in the serum after various treatments (n = 5). Statistical difference was calculated using a two-tailed unpaired student's t-test. Data were expressed as means ± SD. $^{*}P < 0.05$, $^{**}P < 0.01$, and $^{***}P < 0.001$. DPPC: 1,2-dipalmitoyl-*sn*-glycero-3-phosphorylcholine; CHOL: cholesterol; RBC: red blood cell; G1: control; G2: RBC-Alipo; G3: MDCa; G4: MDCa@RBC-Alipo. Reproduced from Ref [183] with permission.

Table 3
Summary of the combination of nanocarriers and tumor ablation technology.

Combination strategy	Ablation technique	Nanocarrier functions and advantages	Main outcomes achieved	Refs.
Targeted therapy for residual tumors at the ablation periphery	RFA, MWA	Active targeting: inhibition of local recurrence and distant metastasis; drug-loaded NPs surface-modified with targeting ligands specifically recognize and bind to residual tumor cells activated by ablation	Increases local drug concentration; enhances killing of residual foci; reduces systemic toxicity	[62,198]
Alleviating tumor hypoxia to enhance chemo/radiotherapy efficacy	RFA, MWA	Oxygen-carrying/oxygen-generating: uses oxygen-carrying carriers to improve the hypoxic microenvironment in the peripheral zone post-ablation; enhances cytotoxicity of chemotherapeutic drugs and efficacy of radiotherapy	Reverses hypoxia; overcomes tumor resistance to chemotherapy and radiotherapy; sensitizes subsequent treatments	[63,118]
Synergistic induction of ICD	All ablation techniques	Immunoadjuvant: inhibition of distant metastatic growth, establishment of immune memory; nanocarriers co-loaded with chemotherapeutic/immunotherapeutic drugs; ablation releases tumor antigens, NPs promote antigen presentation and T-cell activation	Amplifies the "*in-situ* vaccine" effect of ablation, elicits potent systemic antitumor immunity	[127,215,221,236]
Visual guidance and treatment monitoring	RFA	Multifunctional nano-platform: integrates imaging agents; enables precise "see and treat" approach, improves treatment completeness and success rate	Precise tumor localization pre-operation; real-time guidance during ablation; post-operative efficacy assessment and targeted delivery to residual lesions	[119]
Enhancing the ablation effect itself	All ablation techniques	Photothermal conversion agents: uses nanocarriers with high photothermal conversion efficiency; more thorough tumor ablation, clearer treatment margins	Reduces required laser power; improves localization and efficiency of hyperthermia; minimizes damage to normal tissue	[63,97,183,221]

strategies discussed herein are systematically summarized in Table 3 [62,63,97,118,119,127,183,198,215,221,236], which categorizes different nanocarrier ablation approaches on the basis of their therapeutic goals.

This summary highlights the versatility of nanocarrier platforms in addressing the specific limitations of each ablation modality and provides a framework for selecting appropriate combination strategies on the basis of clinical needs (see Table 4 [62,63,118,119,146,176,183,198,211,221] for a schematic overview of the quantitative efficacy metrics of representative nanocarrier-ablation combination platforms).

5. Conclusions and perspectives

The convergence of nanocarrier technology with tumor ablation therapy has presented transformative opportunities for cancer treatment by addressing the fundamental limitations of ablation alone—incomplete eradication, local recurrence, and an iTME. Throughout this review, we highlighted three synergistic mechanisms underlying this integrated approach: amplification of ICD to increase tumor immunogenicity [126,184]; reprogramming of the iTME, including macrophage repolarization and hypoxia alleviation [110,117,129]; and promotion of ablation-triggered antigen presentation, converting the ablation site into an *in situ* vaccine that primes systemic antitumor immunity [95,189,235].

Despite remarkable outcomes in preclinical studies, the clinical translation of nanocarrier-enhanced ablation therapies faces formidable barriers. Thermal ablation induces coagulative necrosis and microvascular disruption, creating a heterogeneous perfusion landscape that may impede nanocarrier delivery to the critical ablation margin [36,37]. Furthermore, the acute inflammatory response from necrotic tissue activates the mononuclear phagocyte system, potentially accelerating nanocarrier clearance and shortening its half-life in circulation [74,237]. These effects, combined with an altered protein corona influenced by systemic inflammation, can lead to off-target effects and unpredictable efficacy [236]. Additionally, ablation of large tumors can induce systemic inflammatory response syndrome (SIRS), increasing the levels of cytokines such as IL-6 and TNF-α [36]. Introducing nanocarriers designed to activate DCs, trigger pyroptosis, or induce trained immunity into this inflamed environment results in a non-negligible risk of inducing a cytokine storm [95,110,235]. This danger is especially acute for agents engaging innate immune pathways, such as STING agonists, where the threshold for safe immune activation may be substantially lower in postablation patients—a nuance seldom addressed in preclinical studies [117,185].

Beyond the risk of inducing an acute cytokine storm, a more insidious concern lies in the potential for nanocarrier–ablation combinations to inadvertently reinforce, rather than reverse, immunosuppressive mechanisms. Sublethal thermal stress at the ablation margin can activate autophagy and heat shock protein pathways that increase residual tumor cell survival while simultaneously recruiting immunosuppressive cells such as MDSCs and Tregs into the periablational zone [177,179]. Moreover, the selective pressure exerted by robust immunostimulatory intervention may drive the emergence of tumor clones with compromised antigen presentation or increased resistance to cell death pathways such as ferroptosis and pyroptosis [180]. These biological risks are distinct from the physical and nonspecific toxicity barriers noted above, and they warrant systematic investigation in future translational studies.

Beyond these ablation-specific challenges, the systemic delivery efficiency of NPs remains a critical limitation. Delivery efficiency is influenced by complex nano–bio interactions and the physicochemical properties of NPs, such as their size, shape, and surface characteristics, which ultimately determine the EPR effect and therapeutic efficacy [238]. Furthermore, the remarkable efficacy observed in murine models often fails to translate to patients, reflecting fundamental differences in tumor biology, immune system complexity, and physiological responses [74,239,240].

In this context, the rapid advancement of artificial intelligence (AI) and machine learning offers unprecedented multidimensional opportunities to address the key translational bottlenecks highlighted in this review, reshaping the research paradigm of nanoablation therapies.

Machine learning models can analyze vast amounts of material science and nano–bio interaction data to establish accurate structure activity relationship models and predict NP physicochemical properties, protein corona composition, tumor accumulation efficiency, and *in vivo* fate [241,242]. AI algorithms can decipher complex high-throughput data to reveal nonlinear relationships

Table 4
Quantitative efficacy metrics of representative nanocarrier-ablation combination platforms.

Nanocarrier platform	Ablation modality	Key quantitative outcomes	Ref.
MFMP (nano-epidrug)	RFA	3.2-Fold increase in tumor-infiltrating $CD8^+$ T cells; 60% reduction in PD-L1 expression; 85% tumor growth inhibition	[118]
PML@Len (PD-1 macrophage membrane-coated vesicles)	RFA	Recurrence rate reduced from 65% to 19% (70% reduction); median survival extended from 38 to 62 days; 4.5-fold increase in $CD8^+$ T cell infiltration; 55% reduction in Tregs	[198]
Fatty acid-binding protein 5-targeting SPIO nanocarrier (sS@RBCM/cRGD-phLips)	RFA	92% tumor volume inhibition; 75% complete ablation rate; 5.2-fold increase in CTL infiltration; 3.8-fold increase in IFN-γ^+CD8^+ T cells	[119]
DA-COD-OD-HCS (cholesterol-targeting catalytic hydrogel)	MWA	88% primary tumor growth inhibition; 90% reduction in distant metastasis; 6.1-fold increase in tumor-infiltrating $CD8^+$ T cells; 4.3-fold increase in TNF-α^+CD8^+ T cells	[62]
Metal-alginate hydrogel (Mn^{2+}/Ca^{2+})	MWA	2.3-Fold larger ablation zone; 60% complete response rate; 4.8-fold STING pathway activation; 5.2-fold increase in IFN-β	[63]
GAT MW-immunosensitizers	MWA	100% tumor inhibition; intratumoral $CD8^+$ T cells increased from 16.8% to 33.2%; effective inhibition of lung metastasis	[211]
DOX@FRMSN-O_2 (protein corona-detachable MWA amplifier)	MWA	Median survival extended beyond 40 days (vs < 20 days for control)	[146]
BMCPH (bi-MOF H_2S immunomodulator)	MWA	6-Fold increase in intratumoral $CD8^+$ T cells; effective reduction of lung metastases; long-term tumor suppression	[176]
MDCa@RBC-Alipo (spleen-targeting nanobiologic)	IRE	320% enhancement of peripheral trained immune responses; median survival extended from 41 to 68 days; 85% reduction in metastasis	[183]
CM NAs (Ce6-mitoxantrone NA)	Phototherapy (PTT/PDT)	94% tumor volume reduction; 50% complete regression; 3.5-fold increase in CRT exposure; 4.1-fold increase in HMGB1 release	[221]

between NP surface properties (e.g., ligand density and spatial conformation) and biological systems (e.g., immune cell uptake and protein adsorption) [243]. By integrating omics data and systems biology approaches, AI can help predict and circumvent off-target effects and immunotoxicity, which is crucial for designing safer, more biocompatible nanoplatforms.

AI can integrate multidimensional, multimodal data spanning genomics, proteomics, radiomics, and clinical records to construct powerful predictive models. These models can identify patient subgroups that are most likely to benefit from specific nanoablation combinations and predict individual treatment responses and potential toxicity risks [244,245]. For example, by analyzing pretreatment tumor biopsy pathology images and gene expression profiles, AI can accurately determine the tumor immune microenvironment type (“cold” or “hot”), guiding the selection of nanocarrier strategies focused on immune activation versus microenvironment remodeling and enabling true personalized therapy.

By combining radiomics and deep learning, AI analyze intraprocedural imaging data (e.g., ultrasound, CT, and MRI) in real time, accurately assess ablation margins, identify potential residual disease tissue, and provide precise spatiotemporal feedback for the on-demand activation of ablation-responsive nanocarriers [2]. Ultimately, this multifaceted, deep convergence will propel the field of nanoablation from an empirical exploration model toward a new era of AI-driven, predictive, data-driven personalized precision therapy.

The rapid advancement of organoid technology provides physiologically relevant platforms for nanocarrier research, with patient-derived tumor organoids uniquely retaining their original tumor heterogeneity and microenvironmental architecture to enable clinically relevant nanocarrier screening predictions [246–248]. Integrating nanocarrier systems with organoid-on-a-chip technology allows *in vitro* reconstruction of the postablation microenvironment, facilitating simulations of nanocarrier behavior at the ablation margin and systematic evaluation of ICD through immune–tumor cocultures [247]. This organoid-guided paradigm accelerates the translation of nanocarrier innovations from bench to bedside, advancing precision nanomedicine for tumor ablation [249].

Bridging the gap from “proof-of-concept” to “clinical translation” represents the central challenge currently faced by the field of nanocarrier-enhanced tumor ablation. On the basis of a systematic elucidation of the spatiotemporal evolution of the postablation TME and a comparative analysis of immune remodeling mechanisms between thermal and nonthermal ablation modalities, we propose three priority research directions for the next decade, aiming to translate mechanistic discoveries into preclinical research frameworks with clear pathways for validation.

We hypothesize that biomaterials engineered to respond directly to ablation-specific stimuli, such as the rapid increase in temperature during RFA/MWA, ice crystal formation during Cryo, or high-voltage electrical pulses during IRE, could enable precise, spatiotemporally controlled drug release, addressing the key bottleneck of the temporal disconnect between ablation and drug activation [195,250,251]. Building on this foundation, closed-loop systems that integrate real-time imaging feedback and use MRI thermometry or functional imaging to dynamically identify residual viable tumors at the ablation margin and precisely trigger nanocarrier activation hold promise for achieving more complete local tumor control and reducing off-target toxicity [37,252]. Realizing this aim relies on two key enabling technologies: real-time TME sensors capable of reporting critical indicators such as hypoxia levels, pH fluctuations, and DAMP release kinetics [253,254]; and multimodal imaging contrast agents that enable simultaneous physical monitoring of the ablation process and biological tracking of nanocarriers within a single platform, achieving a holistic visualization of the therapeutic process [93,215].

Given the fundamental differences in the postablation TME between thermal (e.g., RFA/MWA) and nonthermal (e.g., IRE/Cryo) ablation approaches, including hypoxia levels, ICD characteristics, and inflammatory response kinetics, a “tailored” nanocarrier design is needed [37,59,224]. Specific testable hypotheses include the following: For RFA/MWA, nanocarriers prioritizing hypoxia relief and ferroptosis induction will achieve superior outcomes compared with those focused solely on ICD amplification [119,156]; for IRE/Cryo, nanocarriers that amplify ICD signals and induce trained immunity will outperform those designed primarily for hypoxia relief [183,235]; and furthermore, the optimal timing of nanocarrier administration differs by modality [179]. Achieving this goal is highly dependent on predictive computational models—physiologically based pharmacokinetic models integrating ablation physics, nanocarrier pharmacokinetics/pharmacodynamics, and host immune dynamics—enabling high-throughput

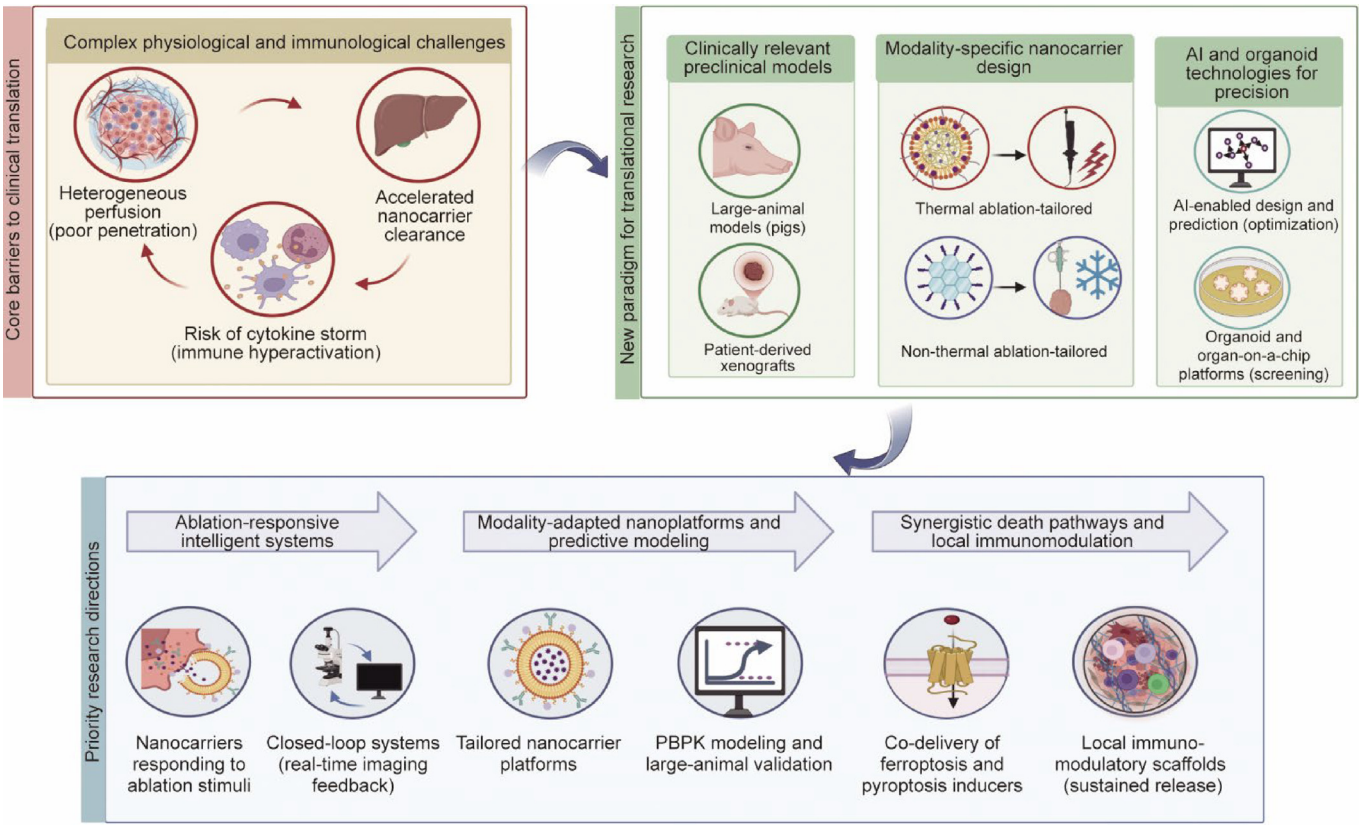

Fig. 10. A systematic overview of nanocarrier-tumor ablation integration barriers and future directions. PBPK: physiologically based pharmacokinetics.

screening and optimization of different ablation–nanocarrier combinations before animal studies [239,255], as well as clinically relevant large-animal models to evaluate nanocarrier biodistribution, efficacy, and safety under conditions resembling those of human disease [256,257].

Nanocarriers codelivering ferroptosis inducers (e.g., iron-based nanomaterials) and pyroptosis primers (e.g., STING agonists) are hypothesized to achieve synergistic antitumor effects and durable immune memory in ablation-resistant tumor models by engaging complementary and synergistic death pathways and creating a more immunogenic TME [112]. Furthermore, implantable or injectable biomaterial scaffolds placed directly in the ablation cavity could serve as local depots for sustained immunomodulation, releasing immune checkpoint inhibitors, cytokines, or personalized neoantigen vaccines over weeks to months, thereby converting the immunologically "cold" ablation site into a "training ground" for priming and launching systemic antitumor immunity, effectively preventing local recurrence and distant metastasis caused by minimal residual disease [62].

The field of nanocarrier-enhanced tumor ablation stands at a critical juncture. The remarkable preclinical successes reviewed here have provided proof-of-concept examples and identified powerful synergistic mechanisms. However, the very biological processes that make these combinations potent—immunostimulation, cell death amplification, and microenvironmental modulation—also carry the risk of unpredictable toxicity when administered to the complex, inflamed environment of a postablation patient. By pursuing the three research directions outlined above—ablation-responsive materials with closed-loop imaging guidance, modality-tailored nanocarrier design, and multitarget combinations to overcome resistance—the field can navigate the steep path from promising preclinical platforms to safe and effective clinical modalities [255]. Only through such a balanced, critical approach can the full potential of this synergistic strategy be realized. The ultimate goal remains clear: to convert focal ablation procedures into personalized, systemic cancer cures (see Fig. 10 for a systematic overview of nanocarrier–tumor ablation integration barriers and future directions).

CRediT authorship contribution statement

Jinhua Luo: Writing – review & editing, Writing – original draft, Visualization, Validation, Software, Resources, Project administration, Methodology, Investigation, Formal analysis, Data curation, Conceptualization. **Bufu Tang:** Writing – review & editing, Writing – original draft, Visualization, Validation, Supervision, Software, Resources, Project administration, Methodology, Investigation, Formal analysis, Data curation, Conceptualization. **Xiaojie Zhang:** Writing – original draft, Visualization, Methodology, Formal analysis, Data curation. **Yun Hu:** Visualization, Validation, Formal analysis, Data curation, Conceptualization. **Shiji Fang:** Validation, Data curation. **Yang Yang:** Validation, Data curation, Conceptualization. **Gaofeng Shu:** Formal analysis, Data curation, Conceptualization. **Jingjing Song:** Data curation, Conceptualization. **Zhongwei Zhao:** Data curation, Conceptualization. **Hamid Reza Karimi:** Data curation, Conceptualization. **Minjiang Chen:** Supervision, Funding acquisition, Conceptualization. **Jiansong Ji:** Supervision, Funding acquisition.

Declaration of competing interest

The authors declare that they have no known competing financial interests or personal relationships that could have appeared to influence the work reported in this paper.

Acknowledgments

This work was supported by the National Natural Science Foundation of China (82072025, 82072026, 82102162, and 82303886), the "Leading Goose" Research and Development Program of Zhejiang Province (2023C03062), the National Natural Science Foundation of Zhejiang Province (LY22H160040 and LQ22H180010), and the Key Research and Development Project of Lishui City (2022ZDYF12, 2022ZDYF20, and 2022ZDYF20).

References

[1] Cooper IS, Lee AS. Cryostatic congelation: a system for producing a limited, controlled region of cooling or freezing of biologic tissues. J Nerv Ment Dis 1961;133:259–63.
[2] Sugiura N, Takara K, Ohto M, Okuda K, Hirroka N. Treatment of small hepatocellular carcinoma by percutaneous injection of ethanol into tumor with real-time ultrasound monitoring. Acta Hepatol Jpn 1983;24:920.
[3] Rossi S, Fornari F, Buscarini L. Percutaneous ultrasound-guided radiofrequency electrocautery for the treatment of small hepatocellular carcinoma. J Interv Radiol 1993;8:97–103.
[4] Seki T, Wakabayashi M, Nakagawa T, Itho T, Shiro T, Kunieda K, et al. Ultrasonically guided percutaneous microwave coagulation therapy for small hepatocellular carcinoma. Cancer 1994;74(3):817–25.
[5] Yi CA, Lee HY, Kim TJ, Lee KS. Management of CT screening-detected persistent nonsolid pulmonary nodules: an Asian perspective. Radiology 2016;280(1):324–6.
[6] Cornelis FH, Solomon SB. Treatment of primary liver tumors and liver metastases, part 2: non-nuclear medicine techniques. J Nucl Med 2018;59 (12):1801–8.
[7] Knavel EM, Brace CL. Tumor ablation: common modalities and general practices. Tech Vasc Interv Radiol 2013;16(4):192–200.
[8] Ahmed M, Brace CL, Lee Jr FT, Goldberg SN. Principles of and advances in percutaneous ablation. Radiology 2011;258(2):351–69.
[9] Livraghi T, Solbiati L, Meloni MF, Gazelle GS, Halpern EF, Goldberg SN. Treatment of focal liver tumors with percutaneous radio-frequency ablation: complications encountered in a multicenter study. Radiology 2003;226 (2):441–51.
[10] Gervais DA, McGovern FJ, Arellano RS, McDougal WS, Mueller PR. Renal cell carcinoma: clinical experience and technical success with radio-frequency ablation of 42 tumors. Radiology 2003;226(2):417–24.
[11] Fan L, Lin Y, Fu Y, Wang J. Small cell lung cancer with liver metastases: from underlying mechanisms to treatment strategies. Cancer Metastasis Rev 2024;44(1):5.
[12] Shimada K, Sakamoto Y, Esaki M, Kosuge T. Role of the width of the surgical margin in a hepatectomy for small hepatocellular carcinomas eligible for percutaneous local ablative therapy. Am J Surg 2008;195(6):775–81.
[13] Gillams A, Cassoni A, Conway G, Lees W. Radiofrequency ablation of neuroendocrine liver metastases: the Middlesex experience. Abdom Imaging 2005;30(4):435–41.
[14] Lencioni R, Cioni D, Crocetti L, Franchini C, Pina CD, Lera J, et al. Early-stage hepatocellular carcinoma in patients with cirrhosis: long-term results of percutaneous image-guided radiofrequency ablation. Radiology 2005;234 (3):961–7.
[15] Seror O. Ablative therapies: advantages and disadvantages of radiofrequency, cryotherapy, microwave and electroporation methods, or how to choose the right method for an individual patient? Diagn Interv Imaging 2015;96 (6):617–24.
[16] Karanicolas PJ, Jarnagin WR, Gonen M, Tuorto S, Allen PJ, DeMatteo RP, et al. Long-term outcomes following tumor ablation for treatment of bilateral colorectal liver metastases. JAMA Surg 2013;148(7):597–601.
[17] Yi Y, Zhang Y, Wei Q, Zhao L, Han J, Song Y, et al. Radiofrequency ablation or microwave ablation combined with transcatheter arterial chemoembolization in treatment of hepatocellular carcinoma by comparing with radiofrequency ablation alone. Chin J Cancer Res 2014;26(1):112–8.
[18] Facciorusso A, Di Maso M, Muscatiello N. Microwave ablation versus radiofrequency ablation for the treatment of hepatocellular carcinoma: a systematic review and meta-analysis. Int J Hyperthermia 2016;32(3):339–44.
[19] Simon CJ, Dupuy DE, Mayo-Smith WW. Microwave ablation: principles and applications. Radiographics 2005;25(Suppl 1):S69–83.
[20] Lubner MG, Brace CL, Hinshaw JL, Lee Jr FT. Microwave tumor ablation: mechanism of action, clinical results, and devices. J Vasc Interv Radiol 2010;21(8 Suppl):S192–203.
[21] Vogl TJ, Nour-Eldin NA, Hammerstingl RM, Panahi B, Naguib NNN. Microwave ablation (MWA): basics, technique and results in primary and metastatic liver neoplasms—review article. Rofo 2017;189(11):1055–66.
[22] Sidoff L, Dupuy DE. Clinical experiences with microwave thermal ablation of lung malignancies. Int J Hyperthermia 2017;33(1):25–33.
[23] Yu Q, Liu C, Navuluri R, Ahmed O. Percutaneous microwave ablation versus radiofrequency ablation of hepatocellular carcinoma: a meta-analysis of randomized controlled trials. Abdom Radiol 2021;46(9):4467–75.
[24] Iezzi R, Cioni R, Basile D, Tosoratti N, Posa A, Busso M, et al. Standardizing percutaneous microwave ablation in the treatment of lung tumors: a prospective multicenter trial (MALT study). Eur Radiol 2021;31(4):2173–82.
[25] Nault JC, Sutter O, Nahon P, Ganne-Carrié N, Séror O. Percutaneous treatment of hepatocellular carcinoma: state of the art and innovations. J Hepatol 2018;68(4):783–97.
[26] Kurilova I, Gonzalez-Aguirre A, Beets-Tan RG, Erinjeri J, Petre EN, Gonen M, et al. Microwave ablation in the management of colorectal cancer pulmonary metastases. Cardiovasc Intervent Radiol 2018;41(10):1530–44.
[27] Amoils SP. The Joule Thomson cryoprobe. Arch Ophthalmol 1967;78 (2):201–7.
[28] Thurlow PC, Azhideh A, Ho CK, Stratchko LM, Pooyan A, Alipour E, et al. Thermal protection techniques for image-guided musculoskeletal ablation. Radiographics 2025;45(4):e240078.
[29] Georgiades CS, Hong K, Bizzell C, Geschwind JF, Rodriguez R. Safety and efficacy of CT-guided percutaneous cryoablation for renal cell carcinoma. J Vasc Interv Radiol 2008;19(9):1302–10.
[30] Orkut S, De Marini P, Tan ASM, Garnon J, Koch G, Tricard T, et al. Profile and methodology of ancillary protective measures employed during percutaneous renal cryoablation in a single high-volume centre. Radiol Med 2025;130(4):493–507.
[31] Zondervan PJ, Buijs M, de la Rosette JJ, van Delden O, van Lienden K, Laguna MP. Cryoablation of small kidney tumors. Int J Surg 2016;36(Pt C):533–40.
[32] Zargar H, Atwell TD, Cadeddu JA, de la Rosette JJ, Janetschek G, Kaouk JH, et al. Cryoablation for small renal masses: selection criteria, complications, and functional and oncologic results. Eur Urol 2016;69(1):116–28.
[33] Dupuy DE, Hong R, Oliver B, Goldberg SN. Radiofrequency ablation of spinal tumors: temperature distribution in the spinal canal. AJR Am J Roentgenol 2000;175(5):1263–6.
[34] Callstrom MR, Charboneau JW. Image-guided palliation of painful metastases using percutaneous ablation. Tech Vasc Interv Radiol 2007;10(2):120–31.
[35] Swarm RA, Paice JA, Anghelescu DL, Are M, Bruce JY, Buga S, et al. the BCPS. Adult cancer pain, version 3.2019, NCCN clinical practice guidelines in oncology. J Natl Compr Canc Netw 2019;17(8):977–1007.
[36] Ahmed M, Solbiati L, Brace CL, Breen DJ, Callstrom MR, Charboneau JW, et al. the International Working Group on Image-guided Tumor Ablation, the Interventional Oncology Sans Frontières Expert Panel, the Technology Assessment Committee of the Society of Interventional Radiology, Standard of Practice Committee of the Cardiovascular and Interventional Radiological Society of Europe. Image-guided tumor ablation: standardization of terminology and reporting criteria—a 10-year update. Radiology 2014;273 (1):241–60.
[37] Chu KF, Dupuy DE. Thermal ablation of tumours: biological mechanisms and advances in therapy. Nat Rev Cancer 2014;14(3):199–208.
[38] Sloan AE, Ahluwalia MS, Valerio-Pascua J, Manjila S, Torchia MG, Jones SE, et al. Results of the NeuroBlate system first-in-humans phase I clinical trial for recurrent glioblastoma: clinical article. J Neurosurg 2013;118 (6):1202–19.
[39] Rahmathulla G, Recinos PF, Kamian K, Mohammadi AM, Ahluwalia MS, Barnett GH. MRI-guided laser interstitial thermal therapy in neuro-oncology: a review of its current clinical applications. Oncology 2014;87(2):67–82.
[40] Scheffer HJ, Nielsen K, de Jong MC, van Tilborg AA, Vieveen JM, Bouwman AR, et al. Irreversible electroporation for nonthermal tumor ablation in the clinical setting: a systematic review of safety and efficacy. J Vasc Interv Radiol 2014;25(7):997–1011. quiz 1011.
[41] Xia ZY, Xiang JC, Xu JZ, Sun JX, Wang S, Xia QD. Irreversible electroporation synergizes with oncolytic virus enhances the infiltration of cytotoxic T lymphocytes in the tumor immune microenvironment: a leap from focal therapy to immunotherapy for prostate cancer. J Immunother Cancer 2025;13(4):e009794.
[42] Kowalczyk KJ, Choueiri TK, Hevelone ND, Trinh QD, Lipsitz SR, Nguyen PL, et al. Comparative effectiveness, costs and trends in treatment of small renal masses from 2005 to 2007. BJU Int 2013;112(4):E273–80.
[43] Goldberg SN, Gazelle GS, Mueller PR. Thermal ablation therapy for focal malignancy: a unified approach to underlying principles, techniques, and diagnostic imaging guidance. AJR Am J Roentgenol 2000;174(2):323–31.
[44] Brace CL. Radiofrequency and microwave ablation of the liver, lung, kidney, and bone: what are the differences? Curr Probl Diagn Radiol 2009;38 (3):135–43.
[45] Vogl TJ, Farshid P, Naguib NN, Zangos S. Thermal ablation therapies in patients with breast cancer liver metastases: a review. Eur Radiol 2013;23 (3):797–804.
[46] Buy X, Tok CH, Szwarc D, Bierry G, Gangi A. Thermal protection during percutaneous thermal ablation procedures: interest of carbon dioxide dissection and temperature monitoring. Cardiovasc Intervent Radiol 2009;32(3):529–34.
[47] Diehn FE, Neeman Z, Hvizda JL, Wood BJ. Remote thermometry to avoid complications in radiofrequency ablation. J Vasc Interv Radiol 2003;14 (12):1569–76.
[48] Ahmed M, Liu Z, Afzal KS, Weeks D, Lobo SM, Kruskal JB, et al. Radiofrequency ablation: effect of surrounding tissue composition on coagulation necrosis in a canine tumor model. Radiology 2004;230(3):761–7.
[49] Goldberg SN, Gazelle GS, Compton CC, Mueller PR, Tanabe KK. Treatment of intrahepatic malignancy with radiofrequency ablation: radiologic–pathologic correlation. Cancer 2000;88(11):2452–63.

[50] Moreira P, Tuncali K, Tempany CM, Tokuda J. The impact of placement errors on the tumor coverage in MRI-guided focal cryoablation of prostate cancer. Acad Radiol 2021;28(6):841–8.
[51] Tokuda J, Wang Q, Tuncali K, Seethamraju RT, Tempany CM, Schmidt EJ. Temperature-sensitive frozen-tissue imaging for cryoablation monitoring using STIR-UTE MRI. Invest Radiol 2020;55(5):310–7.
[52] Georgiades C, Rodriguez R, Azene E, Weiss C, Chaux A, Gonzalez-Roibon N, et al. Determination of the nonlethal margin inside the visible "ice-ball" during percutaneous cryoablation of renal tissue. Cardiovasc Intervent Radiol 2013;36(3):783–90.
[53] Livraghi T, Meloni F, Di Stasi M, Rolle E, Solbiati L, Tinelli C, et al. Sustained complete response and complications rates after radiofrequency ablation of very early hepatocellular carcinoma in cirrhosis: is resection still the treatment of choice? Hepatology 2008;47(1):82–9.
[54] Yang X, Ye X, Zheng A, Huang G, Ni X, Wang J, et al. Percutaneous microwave ablation of stage I medically inoperable non-small cell lung cancer: clinical evaluation of 47 cases. J Surg Oncol 2014;110(6):758–63.
[55] Wolf FJ, Grand DJ, Machan JT, Dipetrillo TA, Mayo-Smith WW, Dupuy DE. Microwave ablation of lung malignancies: effectiveness, CT findings, and safety in 50 patients. Radiology 2008;247(3):871–9.
[56] Zheng K, Wang X. Techniques and status of hepatic arterial infusion chemotherapy for primary hepatobiliary cancers. Ther Adv Med Oncol 2024;16:17588359231225040.
[57] Kim PN, Choi D, Rhim H, Rha SE, Hong HP, Lee J, et al. Planning ultrasound for percutaneous radiofrequency ablation to treat small (≤ 3 cm) hepatocellular carcinomas detected on computed tomography or magnetic resonance imaging: a multicenter prospective study to assess factors affecting ultrasound visibility. J Vasc Interv Radiol 2012;23(5):627–34.
[58] Dodd 3rd GD, Frank MS, Aribandi M, Chopra S, Chintapalli KN. Radiofrequency thermal ablation: computer analysis of the size of the thermal injury created by overlapping ablations. AJR Am J Roentgenol 2001;177(4):777–82.
[59] Davalos RV, Mir IL, Rubinsky B. Tissue ablation with irreversible electroporation. Ann Biomed Eng 2005;33(2):223–31.
[60] Nolsøe CP, Torp-Pedersen S, Burcharth F, Horn T, Pedersen S, Christensen NE, et al. Interstitial hyperthermia of colorectal liver metastases with a US-guided Nd-YAG laser with a diffuser tip: a pilot clinical study. Radiology 1993;187(2):333–7.
[61] Li X, Lovell JF, Yoon J, Chen X. Clinical development and potential of photothermal and photodynamic therapies for cancer. Nat Rev Clin Oncol 2020;17(11):657–74.
[62] Shen L, Yang Z, Zhong Y, Bi Y, Yu J, Lu Q, et al. Cholesterol targeted catalytic hydrogel fueled by tumor debris can enhance microwave ablation therapy and anti-tumor immune response. Adv Sci 2025;12(5):e2406975.
[63] Zhu Y, Yang Z, Pan Z, Hao Y, Wang C, Dong Z, et al. Metallo-alginate hydrogel can potentiate microwave tumor ablation for synergistic cancer treatment. Sci Adv 2022;8(31):eabo5285.
[64] Ferrari M. Cancer nanotechnology: opportunities and challenges. Nat Rev Cancer 2005;5(3):161–71.
[65] Peer D, Karp JM, Hong S, Farokhzad OC, Margalit R, Langer R. Nanocarriers as an emerging platform for cancer therapy. Nat Nanotechnol 2007;2(12):751–60.
[66] Shi J, Votruba AR, Farokhzad OC, Langer R. Nanotechnology in drug delivery and tissue engineering: from discovery to applications. Nano Lett 2010;10(9):3223–30.
[67] Wu P, Han J, Gong Y, Liu C, Yu H, Xie N. Nanoparticle-based drug delivery systems targeting tumor microenvironment for cancer immunotherapy resistance: current advances and applications. Pharmaceutics 2022;14(10):1990.
[68] Li Y, Li XM, Wei LS, Ye JF. Advancements in mitochondrial-targeted nanotherapeutics: overcoming biological obstacles and optimizing drug delivery. Front Immunol 2024;15:1451989.
[69] Nishiyama N. Nanomedicine: nanocarriers shape up for long life. Nat Nanotechnol 2007;2(4):203–4.
[70] Allen TM, Cullis PR. Liposomal drug delivery systems: from concept to clinical applications. Adv Drug Deliv Rev 2013;65(1):36–48.
[71] Barenholz Y. Doxil®—the first FDA-approved nano-drug: lessons learned. J Control Release 2012;160(2):117–34.
[72] Byrne JD, Betancourt T, Brannon-Peppas L. Active targeting schemes for nanoparticle systems in cancer therapeutics. Adv Drug Deliv Rev 2008;60(15):1615–26.
[73] Tenchov R, Bird R, Curtze AE, Zhou Q. Lipid nanoparticles—from liposomes to mRNA vaccine delivery, a landscape of research diversity and advancement. ACS Nano 2021;15(11):16982–7015.
[74] Paramshetti S, Angolkar M, Talath S, Osmani RAM, Spandana A, Al Fatease A, et al. Unravelling the *in vivo* dynamics of liposomes: insights into biodistribution and cellular membrane interactions. Life Sci 2024;346:122616.
[75] Miele E, Spinelli GP, Miele E, Tomao F, Tomao S. Albumin-bound formulation of paclitaxel (Abraxane ABI-007) in the treatment of breast cancer. Int J Nanomedicine 2009;4:99–105.
[76] Gelderblom H, Verweij J, Nooter K, Sparreboom A. Cremophor EL: the drawbacks and advantages of vehicle selection for drug formulation. Eur J Cancer 2001;37(13):1590–8.
[77] Yin H, Kanasty RL, Eltoukhy AA, Vegas AJ, Dorkin JR, Anderson DG. Non-viral vectors for gene-based therapy. Nat Rev Genet 2014;15(8):541–55.
[78] Sercombe L, Veerati T, Moheimani F, Wu SY, Sood AK, Hua S. Advances and challenges of liposome assisted drug delivery. Front Pharmacol 2015;6:286.
[79] Wang J, Tan M, Wang Y, Liu X, Lin A. Advances in modification and delivery of nucleic acid drugs. J Zhejiang Univ, Med Sci 2023;52(4):417–28. Chinese.
[80] Felgner PL, Gadek TR, Holm M, Roman R, Chan HW, Wenz M, et al. Lipofection: a highly efficient, lipid-mediated DNA-transfection procedure. Proc Natl Acad Sci USA 1987;84(21):7413–7.
[81] Akinc A, Maier MA, Manoharan M, Fitzgerald K, Jayaraman M, Barros S, et al. The Onpattro story and the clinical translation of nanomedicines containing nucleic acid-based drugs. Nat Nanotechnol 2019;14(12):1084–7.
[82] Lin KP, Yang CC, Lee YC, Lee MJ, Vest J, Sweetser MT, et al. Patisiran, an RNAi therapeutic for hereditary transthyretin-mediated amyloidosis: sub-analysis in Taiwanese patients from the APOLLO study. J Formos Med Assoc 2024;123(9):975–84.
[83] Hanahan D, Coussens LM. Accessories to the crime: functions of cells recruited to the tumor microenvironment. Cancer Cell 2012;21(3):309–22.
[84] de Visser KE, Joyce JA. The evolving tumor microenvironment: from cancer initiation to metastatic outgrowth. Cancer Cell 2023;41(3):374–403.
[85] Arnol D, Schapiro D, Bodenmiller B, Saez-Rodriguez J, Stegle O. Modeling cell–cell interactions from spatial molecular data with spatial variance component analysis. Cell Rep 2019;29(1):202–211.e6.
[86] Bejarano L, Jordão MJC, Joyce JA. Therapeutic targeting of the tumor microenvironment. Cancer Discov 2021;11(4):933–59.
[87] Han D, Xu Z, Zhuang Y, Ye Z, Qian Q. Current progress in CAR-T cell therapy for hematological malignancies. J Cancer 2021;12(2):326–34.
[88] Binnewies M, Roberts EW, Kersten K, Chan V, Fearon DF, Merad M, et al. Understanding the tumor immune microenvironment (TIME) for effective therapy. Nat Med 2018;24(5):541–50.
[89] Spranger S, Gajewski TF. Impact of oncogenic pathways on evasion of antitumour immune responses. Nat Rev Cancer 2018;18(3):139–47.
[90] He M, Roussak K, Ma F, Borcherding N, Garin V, White M, et al. CD5 expression by dendritic cells directs T cell immunity and sustains immunotherapy responses. Science 2023;379(6633):eabg2752.
[91] Hu J, Arvejeh PM, Bone S, Hett E, Marincola FM, Roh KH. Nanocarriers for cutting-edge cancer immunotherapies. J Transl Med 2025;23(1):447.
[92] Sahu K, Satapathy T, Sahu P, Chandrakar O. Nanocarrier-induced inflammation: mechanisms, immunometabolic impacts and strategies for safer design. TransMed 2026;1(1):100002.
[93] Overchuk M, Zheng G. Overcoming obstacles in the tumor microenvironment: recent advancements in nanoparticle delivery for cancer theranostics. Biomaterials 2018;156:217–37.
[94] Yang M, Li J, Gu P, Fan X. The application of nanoparticles in cancer immunotherapy: targeting tumor microenvironment. Bioact Mater 2020;6(7):1973–87.
[95] Blanco E, Shen H, Ferrari M. Principles of nanoparticle design for overcoming biological barriers to drug delivery. Nat Biotechnol 2015;33(9):941–51.
[96] Prabhakar U, Maeda H, Jain RK, Sevick-Muraca EM, Zamboni W, Farokhzad OC, et al. Challenges and key considerations of the enhanced permeability and retention effect for nanomedicine drug delivery in oncology. Cancer Res 2013;73(8):2412–7.
[97] Yu Z, Wang D, Qi Y, Liu J, Zhou T, Rao W, et al. Autologous-cancer-cryoablation-mediated nanovaccine augments systematic immunotherapy. Mater Horiz 2023;10(5):1661–77.
[98] Liu Y, Qiao L, Zhang S, Wan G, Chen B, Zhou P, et al. Dual pH-responsive multifunctional nanoparticles for targeted treatment of breast cancer by combining immunotherapy and chemotherapy. Acta Biomater 2018;66:310–24.
[99] Luo L, Iqbal MZ, Liu C, Xing J, Akakuru OU, Fang Q, et al. Engineered nano-immunopotentiators efficiently promote cancer immunotherapy for inhibiting and preventing lung metastasis of melanoma. Biomaterials 2019;223:119464.
[100] Gajewski TF, Schreiber H, Fu YX. Innate and adaptive immune cells in the tumor microenvironment. Nat Immunol 2013;14(10):1014–22.
[101] Quail DF, Joyce JA. Microenvironmental regulation of tumor progression and metastasis. Nat Med 2013;19(11):1423–37.
[102] Huang M, Yang X, Li C, Chen H, Pan Y, Chen L, et al. Sepsis-induced PICS: immunometabolic mechanisms, emerging biomarkers, and precision management. TransMed 2026;1(1):100009.
[103] Han S, Wang W, Wang S, Yang T, Zhang G, Wang D, et al. Tumor microenvironment remodeling and tumor therapy based on M2-like tumor associated macrophage-targeting nano-complexes. Theranostics 2021;11(6):2892–916.
[104] Han S, Chi Y, Yang Z, Ma J, Wang L. Tumor microenvironment regulation and cancer targeting therapy based on nanoparticles. J Funct Biomater 2023;14(3):136.
[105] Mantovani A, Marchesi F, Malesci A, Laghi L, Allavena P. Tumour-associated macrophages as treatment targets in oncology. Nat Rev Clin Oncol 2017;14(7):399–416.
[106] De Palma M, Lewis CE. Macrophage regulation of tumor responses to anticancer therapies. Cancer Cell 2013;23(3):277–86.
[107] Sica A, Larghi P, Mancino A, Rubino L, Porta C, Totaro MG, et al. Macrophage polarization in tumour progression. Semin Cancer Biol 2008;18(5):349–55.
[108] Ge W, Wu W. Influencing factors and significance of tumor-associated macrophage polarization in tumor microenvironment. Chin J Lung Cancer 2023;26(3):228–37. Chinese.
[109] Boutilier AJ, Elsawa SF. Macrophage polarization states in the tumor microenvironment. Int J Mol Sci 2021;22(13):6995.

[110] Zanganeh S, Hutter G, Spitler R, Lenkov O, Mahmoudi M, Shaw A, et al. Iron oxide nanoparticles inhibit tumour growth by inducing pro-inflammatory macrophage polarization in tumour tissues. Nat Nanotechnol 2016;11(11):986–94.
[111] Wang M, Pan W, Xu Y, Zhang J, Wan J, Jiang H. Microglia-mediated neuroinflammation: a potential target for the treatment of cardiovascular diseases. J Inflamm Res 2022;15:3083–94.
[112] Ling Y, Liang X, Yan K, Zeng G, Zhu X, Jiang J, et al. Bimetallic Ca/Zn nanoagonist remould the immunosuppressive hepatocellular carcinoma microenvironment following incomplete microwave ablation via pyroptosis and the sting signaling pathway. Adv Sci 2025;12(23):e2500670.
[113] Constantino J, Gomes C, Falcão A, Neves BM, Cruz MT. Dendritic cell-based immunotherapy: a basic review and recent advances. Immunol Res 2017;65(4):798–810.
[114] Maier B, Leader AM, Chen ST, Tung N, Chang C, LeBerichel J, et al. A conserved dendritic-cell regulatory program limits antitumour immunity. Nature 2020;580(7802):257–62.
[115] Gardner A, Ruffell B. Dendritic cells and cancer immunity. Trends Immunol 2016;37(12):855–65.
[116] Luri-Rey C, Teijeira Á, Wculek SK, de Andrea C, Herrero C, Lopez-Janeiro A, et al. Cross-priming in cancer immunology and immunotherapy. Nat Rev Cancer 2025;25(4):249–73.
[117] Liu Q, Zhu H, Liu Y, Musetti S, Huang L. BRAF peptide vaccine facilitates therapy of murine *BRAF*-mutant melanoma. Cancer Immunol Immunother 2018;67(2):299–310.
[118] Li X, Liu Y, Ke J, Wang Z, Han M, Wang N, et al. Enhancing radiofrequency ablation for hepatocellular carcinoma: nano-epidrug effects on immune modulation and antigenicity restoration. Adv Mater 2024;36(52):e2414365.
[119] Tang B, Zhang X, Sun Y, Luo J, Weng Q, Zhang C, et al. Tumor-targeted FABP5/STING cascade promote radiofrequency ablation induced ferroptosis and intratumoral immune rewiring in hepatocellular carcinoma. Adv Sci 2025;12(45):e07864.
[120] Liu YN, Yang JF, Huang DJ, Ni HH, Zhang CX, Zhang L, et al. Hypoxia induces mitochondrial defect that promotes T cell exhaustion in tumor microenvironment through MYC-regulated pathways. Front Immunol 2020;11:1906.
[121] Wherry EJ. T cell exhaustion. Nat Immunol 2011;12(6):492–9.
[122] Chiu DK, Tse AP, Xu IM, Di Cui J, Lai RK, Li LL, et al. Hypoxia inducible factor HIF-1 promotes myeloid-derived suppressor cells accumulation through ENTPD2/CD39L1 in hepatocellular carcinoma. Nat Commun 2017;8(1):517.
[123] Huang L, Zhu J, Xiong W, Feng J, Yang J, Lu X, et al. Tumor-generated reactive oxygen species storm for high-performance ferroptosis therapy. ACS Nano 2023;17(12):11492–506.
[124] Ochoa de Olza M, Navarro Rodrigo B, Zimmermann S, Coukos G. Turning up the heat on non-immunoreactive tumours: opportunities for clinical development. Lancet Oncol 2020;21(9):e419–30.
[125] Chaturvedi P, Gilkes DM, Takano N, Semenza GL. Hypoxia-inducible factor-dependent signaling between triple-negative breast cancer cells and mesenchymal stem cells promotes macrophage recruitment. Proc Natl Acad Sci USA 2014;111(20):E2120–9.
[126] Noman MZ, Desantis G, Janji B, Hasmim M, Karray S, Dessen P, et al. PD-L1 is a novel direct target of HIF-1α, and its blockade under hypoxia enhanced MDSC-mediated T cell activation. J Exp Med 2014;211(5):781–90.
[127] Song J, Wang H, Meng X, Li W, Qi J. A hypoxia-activated and microenvironment-remodeling nanoplatform for multifunctional imaging and potentiated immunotherapy of cancer. Nat Commun 2024;15(1):10395.
[128] Zhou T, Liang X, Wang P, Hu Y, Qi Y, Jin Y, et al. A hepatocellular carcinoma targeting nanostrategy with hypoxia-ameliorating and photothermal abilities that, combined with immunotherapy, inhibits metastasis and recurrence. ACS Nano 2020;14(10):12679–96.
[129] Zhang Y, Li B, He J, Meng Y, Zhan M, Lu C, et al. Hemoglobin-loaded hollow mesoporous carbon-gold nanocomposites enhance microwave ablation through hypoxia relief. J Nanobiotechnology 2025;23(1):326.
[130] Dharmaratne NU, Kaplan AR, Glazer PM. Targeting the hypoxic and acidic tumor microenvironment with pH-sensitive peptides. Cells 2021;10(3):541.
[131] Adochite RC, Moshnikova A, Carlin SD, Guerrieri RA, Andreev OA, Lewis JS, et al. Targeting breast tumors with pH (low) insertion peptides. Mol Pharm 2014;11(8):2896–905.
[132] Demoin DW, Wyatt LC, Edwards KJ, Abdel-Atti D, Sarparanta M, Pourat J, et al. PET imaging of extracellular pH in tumors with ^{64}Cu- and ^{18}F-Labeled pHLIP peptides: a structure-activity optimization study. Bioconjug Chem 2016;27(9):2014–23.
[133] Bergsbaken T, Fink SL, Cookson BT. Pyroptosis: host cell death and inflammation. Nat Rev Microbiol 2009;7(2):99–109.
[134] Min R, Bai Y, Wang NR, Liu X. Gasdermins in pyroptosis, inflammation, and cancer. Trends Mol Med 2025;31(9):860–75.
[135] He WT, Wan H, Hu L, Chen P, Wang X, Huang Z, et al. Gasdermin D is an executor of pyroptosis and required for interleukin-1β secretion. Cell Res 2015;25(12):1285–98.
[136] Shi J, Zhao Y, Wang K, Shi X, Wang Y, Huang H, et al. Cleavage of GSDMD by inflammatory caspases determines pyroptotic cell death. Nature 2015;526(7575):660–5.
[137] Kayagaki N, Stowe IB, Lee BL, O'Rourke K, Anderson K, Warming S, et al. Caspase-11 cleaves gasdermin D for non-canonical inflammasome signalling. Nature 2015;526(7575):666–71.
[138] Wang Y, Gao W, Shi X, Ding J, Liu W, He H, et al. Chemotherapy drugs induce pyroptosis through caspase-3 cleavage of a gasdermin. Nature 2017;547(7661):99–103.
[139] Yu Q, Sun S, Yang N, Pei Z, Chen Y, Nie J, et al. Self-cascaded pyroptosis-STING initiators for catalytic metalloimmunotherapy. J Am Chem Soc 2025;147(4):3161–73.
[140] Zhang Y, Jia Q, Li J, Wang J, Liang K, Xue X, et al. Copper-bacteriochlorin nanosheet as a specific pyroptosis inducer for robust tumor immunotherapy. Adv Mater 2023;35(44):e2305073.
[141] Xiao H, Li X, Liang S, Yang S, Han S, Huang J, et al. Dual-responsive nanomedicine activates programmed antitumor immunity through targeting lymphatic system. ACS Nano 2024;18(17):11070–83.
[142] Chen B, Yan Y, Yang Y, Cao G, Wang X, Wang Y, et al. A pyroptosis nanotuner for cancer therapy. Nat Nanotechnol 2022;17(7):788–98.
[143] Zhang Z, Zhang Y, Xia S, Kong Q, Li S, Liu X, et al. Gasdermin E suppresses tumour growth by activating anti-tumour immunity. Nature 2020;579(7799):415–20.
[144] Wang Q, Wang Y, Ding J, Wang C, Zhou X, Gao W, et al. A bioorthogonal system reveals antitumour immune function of pyroptosis. Nature 2020;579(7799):421–6.
[145] Zhang J, Hu Y, Wen X, Yang Z, Wang Z, Feng Z, et al. Tandem-controlled lysosomal assembly of nanofibres induces pyroptosis for cancer immunotherapy. Nat Nanotechnol 2025;20(4):563–74.
[146] Wang T, Wu Q, Zhu C, Zhang Z, Gu Y, Chang Z, et al. Protein corona-detachable microwave ablation amplifiers actuate pyroptosis to repolarize immortal cancer into senescent ones. ACS Nano 2025;19(32):29577–92.
[147] Yagoda N, von Rechenberg M, Zaganjor E, Bauer AJ, Yang WS, Fridman DJ, et al. RAS-RAF-MEK-dependent oxidative cell death involving voltage-dependent anion channels. Nature 2007;447(7146):864–8.
[148] Liu X, Kim CN, Yang J, Jemmerson R, Wang X. Induction of apoptotic program in cell-free extracts: requirement for dATP and cytochrome C. Cell 1996;86(1):147–57.
[149] Kerr JF, Wyllie AH, Currie AR. Apoptosis: a basic biological phenomenon with wide-ranging implications in tissue kinetics. Br J Cancer 1972;26(4):239–57.
[150] Dixon SJ, Lemberg KM, Lamprecht MR, Skouta R, Zaitsev EM, Gleason CE, et al. Ferroptosis: an iron-dependent form of nonapoptotic cell death. Cell 2012;149(5):1060–72.
[151] Yang WS, SriRamaratnam R, Welsch ME, Shimada K, Skouta R, Viswanathan VS, et al. Regulation of ferroptotic cancer cell death by GPX4. Cell 2014;156(1–2):317–31.
[152] Doll S, Proneth B, Tyurina YY, Panzilius E, Kobayashi S, Ingold I, et al. ACSL4 dictates ferroptosis sensitivity by shaping cellular lipid composition. Nat Chem Biol 2017;13(1):91–8.
[153] Yang WS, Stockwell BR. Synthetic lethal screening identifies compounds activating iron-dependent, nonapoptotic cell death in oncogenic-RAS-harboring cancer cells. Chem Biol 2008;15(3):234–45.
[154] Gaschler MM, Hu F, Feng H, Linkermann A, Min W, Stockwell BR. Determination of the subcellular localization and mechanism of action of ferrostatins in suppressing ferroptosis. ACS Chem Biol 2018;13(4):1013–20.
[155] Jiang X, Stockwell BR, Conrad M. Ferroptosis: mechanisms, biology and role in disease. Nat Rev Mol Cell Biol 2021;22(4):266–82.
[156] Zhang S, Wu X, Liao X, Zhang S. Nanodrug hijacking blood transferrin for ferroptosis-mediated cancer treatment. J Am Chem Soc 2024;146(12):8567–75.
[157] Zhu L, You Y, Zhu M, Song Y, Zhang J, Hu J, et al. Ferritin-hijacking nanoparticles spatiotemporally directing endogenous ferroptosis for synergistic anticancer therapy. Adv Mater 2022;34(51):e2207174.
[158] Feng Y, Chen Q, Jin C, Ruan Y, Chen Q, Lin W, et al. Microwave-activated Cu-doped zirconium metal-organic framework for a highly effective combination of microwave dynamic and thermal therapy. J Control Release 2023;361:102–14.
[159] Liu T, Liu W, Zhang M, Yu W, Gao F, Li C, et al. Ferrous-supply-regeneration nanoengineering for cancer-cell-specific ferroptosis in combination with imaging-guided photodynamic therapy. ACS Nano 2018;12(12):12181–92.
[160] Fu F, Wang W, Wu L, Wang W, Huang Z, Huang Y, et al. Inhalable biomineralized liposomes for cyclic Ca^{2+}-burst-centered endoplasmic reticulum stress enhanced lung cancer ferroptosis therapy. ACS Nano 2023;17(6):5486–502.
[161] Hou W, Hong W, Cai S, Guo D, Yan Z, Zhu J, et al. RRM2-targeted nanocarrier enhances radiofrequency ablation efficacy in hepatocellular carcinoma through ferroptosis amplification and immune remodeling. iMeta 2025;4(5):e70067.
[162] Zhang X, Zhang Y, Lv X, Zhang P, Xiao C, Chen X. DNA-free guanosine-based polymer nanoreactors with multienzyme activities for ferroptosis-apoptosis combined antitumor therapy. ACS Nano 2024;18(49):33531–44.
[163] Zerbini A, Pilli M, Laccabue D, Pelosi G, Molinari A, Negri E, et al. Radiofrequency thermal ablation for hepatocellular carcinoma stimulates autologous NK-cell response. Gastroenterology 2010;138(5):1931–42.
[164] Krysko DV, Garg AD, Kaczmarek A, Krysko O, Agostinis P, Vandenabeele P. Immunogenic cell death and DAMPs in cancer therapy. Nat Rev Cancer 2012;12(12):860–75.
[165] Crosby D, Bhatia S, Brindle KM, Coussens LM, Dive C, Emberton M, et al. Early detection of cancer. Science 2022;375(6586):eaay9040.
[166] Wahida A, Buschhorn L, Fröhling S, Jost PJ, Schneeweiss A, Lichter P, et al. The coming decade in precision oncology: six riddles. Nat Rev Cancer 2023;23(1):43–54.

[167] Chen R, Mias GI, Li-Pook-Than J, Jiang L, Lam HY, Chen R, et al. Personal omics profiling reveals dynamic molecular and medical phenotypes. Cell 2012;148 (6):1293–307.
[168] Kim SY, An J, Lim YS, Han S, Lee JY, Byun JH, et al. MRI with liver-specific contrast for surveillance of patients with cirrhosis at high risk of hepatocellular carcinoma. JAMA Oncol 2017;3(4):456–63.
[169] James ML, Gambhir SS. A molecular imaging primer: modalities, imaging agents, and applications. Physiol Rev 2012;92(2):897–965.
[170] Abd Elkodous M, El-Sayyad GS, Abdelrahman IY, El-Bastawisy HS, Mohamed AE, Mosallam FM, et al. Therapeutic and diagnostic potential of nanomaterials for enhanced biomedical applications. Colloids Surf B Biointerfaces 2019;180:411–28.
[171] Dykman L, Khlebtsov N. Gold nanoparticles in biomedical applications: recent advances and perspectives. Chem Soc Rev 2012;41(6):2256–82.
[172] Chen Y, Xianyu Y, Jiang X. Surface modification of gold nanoparticles with small molecules for biochemical analysis. Acc Chem Res 2017;50(2):310–9.
[173] Keliher EJ, Yoo J, Nahrendorf M, Lewis JS, Marinelli B, Newton A, et al. ^{89}Zr-labeled dextran nanoparticles allow *in vivo* macrophage imaging. Bioconjug Chem 2011;22(12):2383–9.
[174] Wu Q, Tan L, Ren X, Fu C, Chen Z, Ren J, et al. Metal-organic framework-based nano-activators facilitating microwave combined therapy via a divide-and-conquer tactic for triple-negative breast cancer. ACS Nano 2023;17 (24):25575–90.
[175] Zhang S, Xie F, Li K, Zhang H, Yin Y, Yu Y, et al. Gold nanoparticle-directed autophagy intervention for antitumor immunotherapy *via* inhibiting tumor-associated macrophage M2 polarization. Acta Pharm Sin B 2022;12 (7):3124–38.
[176] Li S, Xu F, Ren X, Tan L, Fu C, Wu Q, et al. H_2S-reactivating antitumor immune response after microwave thermal therapy for long-term tumor suppression. ACS Nano 2023;17(19):19242–53.
[177] Zeng X, Liao G, Li S, Liu H, Zhao X, Li S, et al. Eliminating METTL1-mediated accumulation of PMN-MDSCs prevents hepatocellular carcinoma recurrence after radiofrequency ablation. Hepatology 2023;77(4):1122–38.
[178] Nijkamp MW, van der Bilt JD, de Bruijn MT, Molenaar IQ, Voest EE, van Diest PJ, et al. Accelerated perinecrotic outgrowth of colorectal liver metastases following radiofrequency ablation is a hypoxia-driven phenomenon. Ann Surg 2009;249(5):814–23.
[179] Shi L, Wang J, Ding N, Zhang Y, Zhu Y, Dong S, et al. Inflammation induced by incomplete radiofrequency ablation accelerates tumor progression and hinders PD-1 immunotherapy. Nat Commun 2019;10(1):5421.
[180] Shi ZR, Duan YX, Cui F, Wu ZJ, Li MP, Song PP, et al. Integrated proteogenomic characterization reveals an imbalanced hepatocellular carcinoma microenvironment after incomplete radiofrequency ablation. J Exp Clin Cancer Res 2023;42(1):133.
[181] Weiss MJ, Wolfgang CL. Irreversible electroporation: a novel pancreatic cancer therapy. Curr Probl Cancer 2013;37(5):262–5.
[182] Aymeric L, Apetoh L, Ghiringhelli F, Tesniere A, Martins I, Kroemer G, et al. Tumor cell death and ATP release prime dendritic cells and efficient anticancer immunity. Cancer Res 2010;70(3):855–8.
[183] Wu S, Xu W, Shan X, Sun L, Liu S, Sun X, et al. Targeting splenic myeloid cells with nanobiologics to prevent postablative pancreatic cancer recurrence via inducing antitumor peripheral trained immunity. Adv Sci 2025;12(21): e2413562.
[184] Deng X, Shao Z, Zhao Y. Solutions to the drawbacks of photothermal and photodynamic cancer therapy. Adv Sci 2021;8(3):2002504.
[185] Hagiwara S, Nishida N, Kudo M. Advances in immunotherapy for hepatocellular carcinoma. Cancers 2023;15(7):2070.
[186] Izzo F, Thomas R, Delrio P, Rinaldo M, Vallone P, DeChiara A, et al. Radiofrequency ablation in patients with primary breast carcinoma: a pilot study in 26 patients. Cancer 2001;92(8):2036–44.
[187] European Association for the Study of the Liver, the European Organisation for Research and Treatment of Cancer. EASL-EORTC clinical practice guidelines: management of hepatocellular carcinoma. J Hepatol 2012;56 (4):908–43.
[188] Ali MY, Grimm CF, Ritter M, Mohr L, Allgaier HP, Weth R, et al. Activation of dendritic cells by local ablation of hepatocellular carcinoma. J Hepatol 2005;43(5):817–22.
[189] den Brok MH, Sutmuller RP, van der Voort R, Bennink EJ, Figdor CG, Ruers TJ, et al. *In situ* tumor ablation creates an antigen source for the generation of antitumor immunity. Cancer Res 2004;64(11):4024–9.
[190] Shi L, Chen L, Wu C, Zhu Y, Xu B, Zheng X, et al. PD-1 blockade boosts radiofrequency ablation-elicited adaptive immune responses against tumor. Clin Cancer Res 2016;22(5):1173–84.
[191] Zerbini A, Pilli M, Penna A, Pelosi G, Schianchi C, Molinari A, et al. Radiofrequency thermal ablation of hepatocellular carcinoma liver nodules can activate and enhance tumor-specific T-cell responses. Cancer Res 2006;66(2):1139–46.
[192] Widenmeyer M, Shebzukhov Y, Haen SP, Schmidt D, Clasen S, Boss A, et al. Analysis of tumor antigen-specific T cells and antibodies in cancer patients treated with radiofrequency ablation. Int J Cancer 2011;128(11):2653–62.
[193] Chen MS, Li JQ, Zheng Y, Guo RP, Liang HH, Zhang YQ, et al. A prospective randomized trial comparing percutaneous local ablative therapy and partial hepatectomy for small hepatocellular carcinoma. Ann Surg 2006;243 (3):321–38.
[194] Mizukoshi E, Yamashita T, Arai K, Sunagozaka H, Ueda T, Arihara F, et al. Enhancement of tumor-associated antigen-specific T cell responses by radiofrequency ablation of hepatocellular carcinoma. Hepatology 2013;57 (4):1448–57.
[195] Liu Q, Zhang W, Jiao R, Lv Z, Lin X, Xiao Y, et al. Rational nanomedicine design enhances clinically physical treatment-inspired or combined immunotherapy. Adv Sci 2022;9(29):e2203921.
[196] Oroojalian F, Beygi M, Baradaran B, Mokhtarzadeh A, Shahbazi MA. Immune cell membrane-coated biomimetic nanoparticles for targeted cancer therapy. Small 2021;17(12):e2006484.
[197] Zhai Y, Wang J, Lang T, Kong Y, Rong R, Cai Y, et al. T lymphocyte membrane-decorated epigenetic nanoinducer of interferons for cancer immunotherapy. Nat Nanotechnol 2021;16(11):1271–80.
[198] Guo H, Huang G, Long H, Wu W, Lin K, Qiao B, et al. Harnessing PD-1-overexpressing macrophage membrane for preparation of lenvatinib-loaded vesicles to boost immunotherapy against HCC recurrence after radiofrequency ablation. Biomaterials 2025;323:123433.
[199] Takaki H, Imai N, Thomas CT, Yamakado K, Yarmohammadi H, Ziv E, et al. Changes in peripheral blood T-cell balance after percutaneous tumor ablation. Minim Invasive Ther Allied Technol 2017;26(6):331–7.
[200] Yu M, Pan H, Che N, Li L, Wang C, Wang Y, et al. Microwave ablation of primary breast cancer inhibits metastatic progression in model mice via activation of natural killer cells. Cell Mol Immunol 2021;18(9):2153–64.
[201] Leuchte K, Staib E, Thelen M, Gödel P, Lechner A, Zentis P, et al. Microwave ablation enhances tumor-specific immune response in patients with hepatocellular carcinoma. Cancer Immunol Immunother 2021;70 (4):893–907.
[202] Zhou W, Yu M, Pan H, Qiu W, Wang H, Qian M, et al. Microwave ablation induces Th1-type immune response with activation of ICOS pathway in early-stage breast cancer. J Immunother Cancer 2021;9(4):e002343.
[203] Kepp O, Marabelle A, Zitvogel L, Kroemer G. Oncolysis without viruses—inducing systemic anticancer immune responses with local therapies. Nat Rev Clin Oncol 2020;17(1):49–64.
[204] Li L, Wang W, Pan H, Ma G, Shi X, Xie H, et al. Microwave ablation combined with OK-432 induces Th1-type response and specific antitumor immunity in a murine model of breast cancer. J Transl Med 2017;15(1):23.
[205] Yin XY, Xie XY, Lu MD, Xu HX, Xu ZF, Kuang M, et al. Percutaneous thermal ablation of medium and large hepatocellular carcinoma: long-term outcome and prognostic factors. Cancer 2009;115(9):1914–23.
[206] Qin S, Liu GJ, Huang M, Huang J, Luo Y, Wen Y, et al. The local efficacy and influencing factors of ultrasound-guided percutaneous microwave ablation in colorectal liver metastases: a review of a 4-year experience at a single center. Int J Hyperthermia 2019;36(1):36–43.
[207] Xu F, Wei Z, Ye X. Immunomodulatory effects of microwave ablation on malignant tumors. Am J Cancer Res 2024;14(6):2714–30.
[208] Zhu J, Yu M, Chen L, Kong P, Li L, Ma G, et al. Enhanced antitumor efficacy through microwave ablation in combination with immune checkpoints blockade in breast cancer: a pre-clinical study in a murine model. Diagn Interv Imaging 2018;99(3):135–42.
[209] Rangamuwa K, Leong T, Weeden C, Asselin-Labat ML, Bozinovski S, Christie M, et al. Thermal ablation in non-small cell lung cancer: a review of treatment modalities and the evidence for combination with immune checkpoint inhibitors. Transl Lung Cancer Res 2021;10(6):2842–57.
[210] Xing R, Gao J, Cui Q, Wang Q. Strategies to improve the antitumor effect of immunotherapy for hepatocellular carcinoma. Front Immunol 2021;12:783236.
[211] Guo W, Chen Z, Wu Q, Tan L, Ren X, Fu C, et al. Prepared MW-immunosensitizers precisely release no to downregulate HIF-1α expression and enhance immunogenic cell death. Small 2024;20(17):e2308055.
[212] Ma X, Bi E, Lu Y, Su P, Huang C, Liu L, et al. Cholesterol induces $CD8^+$ T cell exhaustion in the tumor microenvironment. Cell Metab 2019;30(1):143–156.e5.
[213] Huang B, Song BL, Xu C. Cholesterol metabolism in cancer: mechanisms and therapeutic opportunities. Nat Metab 2020;2(2):132–41.
[214] Liu X, Bao X, Hu M, Chang H, Jiao M, Cheng J, et al. Inhibition of PCSK9 potentiates immune checkpoint therapy for cancer. Nature 2020;588 (7839):693–8.
[215] Li X, Peng X, Zoulikha M, Boafo GF, Magar KT, Ju Y, et al. Multifunctional nanoparticle-mediated combining therapy for human diseases. Signal Transduct Target Ther 2024;9(1):1.
[216] Krajczewski J, Rucińska K, Townley HE, Kudelski A. Role of various nanoparticles in photodynamic therapy and detection methods of singlet oxygen. Photodiagnosis Photodyn Ther 2019;26:162–78.
[217] Zhao X, Liu J, Fan J, Chao H, Peng X. Recent progress in photosensitizers for overcoming the challenges of photodynamic therapy: from molecular design to application. Chem Soc Rev 2021;50(6):4185–219.
[218] Agostinis P, Berg K, Cengel KA, Foster TH, Girotti AW, Gollnick SO, et al. Photodynamic therapy of cancer: an update. CA Cancer J Clin 2011;61 (4):250–81.
[219] Snyder JW, Greco WR, Bellnier DA, Vaughan L, Henderson BW. Photodynamic therapy: a means to enhanced drug delivery to tumors. Cancer Res 2003;63 (23):8126–31.
[220] Ruan K, Song G, Ouyang G. Role of hypoxia in the hallmarks of human cancer. J Cell Biochem 2009;107(6):1053–62.
[221] Su Q, Wang Z, Zhou H, Zhang M, Deng W, Wei X, et al. Eradication of large tumors by nanoscale drug self-assembly. Adv Mater 2024;36(49):e2410536.
[222] Lim CK, Shin J, Lee YD, Kim J, Oh KS, Yuk SH, et al. Phthalocyanine-aggregated polymeric nanoparticles as tumor-homing near-infrared absorbers for photothermal therapy of cancer. Theranostics 2012;2(9):871–9.

[223] Jiang C, Davalos RV, Bischof JC. A review of basic to clinical studies of irreversible electroporation therapy. IEEE Trans Biomed Eng 2015;62(1):4–20.
[224] Yarmush ML, Golberg A, Serša G, Kotnik T, Miklavčič D. Electroporation-based technologies for medicine: principles, applications, and challenges. Annu Rev Biomed Eng 2014;16(1):295–320.
[225] Onik G, Mikus P, Rubinsky B. Irreversible electroporation: implications for prostate ablation. Technol Cancer Res Treat 2007;6(4):295–300.
[226] Krysko O, Løve Aaes T, Bachert C, Vandenabeele P, Krysko DV. Many faces of DAMPs in cancer therapy. Cell Death Dis 2013;4(5):e631.
[227] Kepp O, Tesniere A, Zitvogel L, Kroemer G. The immunogenicity of tumor cell death. Curr Opin Oncol 2009;21(1):71–6.
[228] Kepp O, Tesniere A, Schlemmer F, Michaud M, Senovilla L, Zitvogel L, et al. Immunogenic cell death modalities and their impact on cancer treatment. Apoptosis 2009;14(4):364–75.
[229] Tesniere A, Panaretakis T, Kepp O, Apetoh L, Ghiringhelli F, Zitvogel L, et al. Molecular characteristics of immunogenic cancer cell death. Cell Death Differ 2008;15(1):3–12.
[230] Apetoh L, Ghiringhelli F, Tesniere A, Obeid M, Ortiz C, Criollo A, et al. Toll-like receptor 4-dependent contribution of the immune system to anticancer chemotherapy and radiotherapy. Nat Med 2007;13(9):1050–9.
[231] Li X, Xu K, Li W, Qiu X, Ma B, Fan Q, et al. Immunologic response to tumor ablation with irreversible electroporation. PLoS One 2012;7(11):e48749.
[232] Neal RE, Rossmeisl Jr JH, Robertson JL, Arena CB, Davis EM, Singh RN, et al. Improved local and systemic anti-tumor efficacy for irreversible electroporation in immunocompetent versus immunodeficient mice. PLoS One 2013;8(5):e64559.
[233] Lewis SM, Williams A, Eisenbarth SC. Structure and function of the immune system in the spleen. Sci Immunol 2019;4(33):eaau6085.
[234] Cheng Q, Wei T, Farbiak L, Johnson LT, Dilliard SA, Siegwart DJ. Selective organ targeting (SORT) nanoparticles for tissue-specific mRNA delivery and CRISPR–Cas gene editing. Nat Nanotechnol 2020;15(4):313–20.
[235] Mulder WJM, Ochando J, Joosten LAB, Fayad ZA, Netea MG. Therapeutic targeting of trained immunity. Nat Rev Drug Discov 2019;18(7):553–66.
[236] Long X, Dai A, Huang T, Niu W, Liu L, Xu H, et al. Simultaneous delivery of dual inhibitors of DNA damage repair sensitizes pancreatic cancer response to irreversible electroporation. ACS Nano 2023;17(13):12915–32.
[237] Luo B, Cheng T, Xiang Y, Sun S, Liu Y, Yan J, et al. Promoting retinal ganglion cell regeneration with targeted liposome-based delivery of MHY1485 for optic nerve repair. J Control Release 2025;383:113778.
[238] Shi J, Kantoff PW, Wooster R, Farokhzad OC. Cancer nanomedicine: progress, challenges and opportunities. Nat Rev Cancer 2017;17(1):20–37.
[239] Yuan D, He H, Wu Y, Fan J, Cao Y. Physiologically based pharmacokinetic modeling of nanoparticles. J Pharm Sci 2019;108(1):58–72.
[240] Guo C, Lin L, Wang Y, Jing J, Gong Q, Luo K. Nano drug delivery systems for advanced immune checkpoint blockade therapy. Theranostics 2025;15(11):5440–80.
[241] Adir O, Poley M, Chen G, Froim S, Krinsky N, Shklover J, et al. Integrating artificial intelligence and nanotechnology for precision cancer medicine. Adv Mater 2020;32(13):e1901989.
[242] Ho D, Wang P, Kee T. Artificial intelligence in nanomedicine. Nanoscale Horiz 2019;4(2):365–77.
[243] Walkey CD, Olsen JB, Song F, Liu R, Guo H, Olsen DW, et al. Protein corona fingerprinting predicts the cellular interaction of gold and silver nanoparticles. ACS Nano 2014;8(3):2439–55.
[244] Sammut SJ, Crispin-Ortuzar M, Chin SF, Provenzano E, Bardwell HA, Ma W, et al. Multi-omic machine learning predictor of breast cancer therapy response. Nature 2022;601(7894):623–9.
[245] Chua IS, Gaziel-Yablowitz M, Korach ZT, Kehl KL, Levitan NA, Arriaga YE, et al. Artificial intelligence in oncology: path to implementation. Cancer Med 2021;10(12):4138–49.
[246] Kratochvil MJ, Seymour AJ, Li TL, Paşca SP, Kuo CJ, Heilshorn SC. Engineered materials for organoid systems. Nat Rev Mater 2019;4(9):606–22.
[247] Veninga V, Voest EE. Tumor organoids: opportunities and challenges to guide precision medicine. Cancer Cell 2021;39(9):1190–201.
[248] Wang Y, Ye Z, Lin Y, Zhao Y, Zhong D, Chen J, et al. The promise and potential of liver organoids: development, classification and application. TransMed 2026;1(1):100003.
[249] Bai L, Reis RL, Chen S, Su J, Liu C. Organoid research: advanced models, precision medicine, and translational medicine. Organoid Res 2025;1(1):25060009.
[250] Bakr E, Elshami FI, Okba EA, Mansour H, Shaban SY. Stimuli-responsive chitosan-coated ferrite nanocarriers for targeted capsaicin delivery and core-dependent HepG2-selective bioactivity. Sci Rep 2026;16(1):8957.
[251] Torchilin VP. Multifunctional, stimuli-sensitive nanoparticulate systems for drug delivery. Nat Rev Drug Discov 2014;13(11):813–27.
[252] Zhu L, Zhou Z, Mao H, Yang L. Magnetic nanoparticles for precision oncology: theranostic magnetic iron oxide nanoparticles for image-guided and targeted cancer therapy. Nanomedicine 2017;12(1):73–87.
[253] Kwong GA, Ghosh S, Gamboa L, Patriotis C, Srivastava S, Bhatia SN. Synthetic biomarkers: a twenty-first century path to early cancer detection. Nat Rev Cancer 2021;21(10):655–68.
[254] Luo Y, Yu Y, Chen Y, Li R, Zhang Y, Chen S. Liquid metal-based biomaterials and flexible devices for injectable and implantable healthcare. Acta Biomater 2025;207:1–33.
[255] Gong Z, Zhou D, Wu D, Han Y, Yu H, Shen H, et al. Challenges and material innovations in drug delivery to central nervous system tumors. Biomaterials 2025;319:123180.
[256] Khanna C, Hunter K. Modeling metastasis *in vivo*. Carcinogenesis 2005;26(3):513–23.
[257] Paoloni M, Khanna C. Translation of new cancer treatments from pet dogs to humans. Nat Rev Cancer 2008;8(2):147–56.